AIR FORCE REPORT NO.
SAMSO-TR-71-337

AEROSPACE REPORT NO.
TR-0172(2129-01)-2, VOL I

The Light Scattering Properties of Clouds

Volume I: Analysis of Experimental Results

Prepared by R. T. HALL and R. D. RAWCLIFFE
Space Physics Laboratory
Laboratory Operations

71 NOV 30

Systems Engineering Operations
THE AEROSPACE CORPORATION

Prepared for SPACE AND MISSILE SYSTEMS ORGANIZATION
AIR FORCE SYSTEMS COMMAND
LOS ANGELES AIR FORCE STATION
Los Angeles, California

94

UNCLASSIFIED
Security Classification

DOCUMENT CONTROL DATA - R & D
(Security classification of title, body of abstract and indexing annotation must be entered when the overall report is classified)

1. ORIGINATING ACTIVITY (Corporate author)	2a. REPORT SECURITY CLASSIFICATION
The Aerospace Corporation El Segundo, California	Unclassified 2b GROUP

3. REPORT TITLE

THE LIGHT SCATTERING PROPERTIES OF CLOUDS
VOLUME I: ANALYSIS OF EXPERIMENTAL RESULTS

4 DESCRIPTIVE NOTES (Type of report and inclusive dates)

5 AUTHOR(S) (First name, middle initial, last name)

Richard T. Hall and R. Douglas Rawcliffe

6 REPORT DATE	7a TOTAL NO. OF PAGES	7b. NO. OF REFS
71 NOV 30	71	16

8a CONTRACT OR GRANT NO.	9a. ORIGINATOR'S REPORT NUMBER(S)
F04701-71-C-0172 b. PROJECT NO.	TR-0172(2129-01)-2, Vol I
c.	9b. OTHER REPORT NO(S) (Any other numbers that may be assigned this report)
d.	SAMSO-TR-71-337

10. DISTRIBUTION STATEMENT

Approved for public release; distribution unlimited.

11. SUPPLEMENTARY NOTES	12. SPONSORING MILITARY ACTIVITY
	Space and Missile Systems Organization Air Force Systems Command Los Angeles, California

13. ABSTRACT

A series of experimental measurements of the visible light angular scattering profiles of clouds is described. The results for single layer overcast clouds were found to correlate well with standard hemispheric and narrow-angle pyreheliometric transmittances. The resulting expression for the angular scattering profile of an overcast cloud layer is:

$$T(\theta) = A + B \sin^2\theta$$

where

$$A = -0.0056 + 0.89 \times T_n$$

$$B = -0.028 + 1.09 \times T_w$$

and θ is the half angle of the field of view, T_n the transmittance measured with a narrow-angle pyrheliometer, and T_w the transmittance measured with a hemispheric pyrheliometer.

DD FORM 1473 (FACSIMILE)

UNCLASSIFIED
Security Classification

14. KEY WORDS
Clouds Transmission Meteorology Scattering
Distribution Statement (Continued)
Abstract (Continued)

Air Force Report No.
SAMSO-TR-71-337

Aerospace Report No.
TR-0172(2129-01)-2, Vol I

THE LIGHT SCATTERING PROPERTIES OF CLOUDS
VOLUME I: ANALYSIS OF EXPERIMENTAL RESULTS

Prepared by

R. T. Hall and R. D. Rawcliffe
Space Physics Laboratory
Laboratory Operations

71 NOV 30

Systems Engineering Operations
THE AEROSPACE CORPORATION

Prepared for

SPACE AND MISSILE SYSTEMS ORGANIZATION
AIR FORCE SYSTEMS COMMAND
LOS ANGELES AIR FORCE STATION
Los Angeles, California

FOREWORD

This report is published by The Aerospace Corporation, El Segundo, California, under Air Force Contract No. F04701-71-C-0172.

This report, which documents research carried out from January 1967 through July 1971, was submitted 3 November 1971 to Lieutenant Colonel Roy C. Robinette, SZD, for review and approval.

The authors would like to thank T. Mott for his assistance in setting up and running the experiment; R. Williams for his help in designing the electronics and data recording systems; Lieutenant Colonel J. Coblenz, B. Walker, and the staff of Detachment 10, 6th Weather Wing, for their assistance and hospitality during the course of the experiment; and Mrs. Gwen Boyd and her staff for their efforts in the transcription of the data onto computer coding sheets.

Approved

J. C. Creswell, Director
Mission Support Office
Group II Programs Directorate
Satellite Systems Division
Systems Engineering Operations

G. A. Paulikas, Director
Space Physics Laboratory
Laboratory Operations

Publication of this report does not constitute Air Force approval of the report's findings or conclusions. It is published only for the exchange and stimulation of ideas.

Roy C. Robinette, Lt. Col., USAF
Director of Test
Defense Support Program

ABSTRACT

A series of experimental measurements of the visible light angular scattering profiles of clouds is described. The results for single layer overcast clouds were found to correlate well with standard hemispheric and narrow-angle pyrheliometric transmittances. The resulting expression for the angular scattering profile of an overcast cloud layer is:

$$T(\theta) = A + B \sin^2\theta$$

where

$$A = -0.0056 + 0.89 \times T_n$$

$$B = -0.028 + 1.09 \times T_w$$

and θ is the half angle of the field of view, T_n the transmittance measured with a narrow-angle pyrheliometer, and T_w the transmittance measured with a hemispheric pyrheliometer.

CONTENTS

FIGURES

TABLES

I. INTRODUCTION AND SUMMARY

The light scattering properties of clouds are of great interest for a variety of reasons. In particular, they have a major impact on the performance of several classes of optical systems for which clouds may serve as a background or foreground. It is important in the understanding of the performance of these systems that the cloud scattering characteristics be known. Many experimental and theoretical studies of cloud scattering have been and are being carried out. However, one important aspect, the angular distribution of the scattered sunlight that penetrates the cloud, has been neglected. In this paper the results of an experimental measurement of this distribution are presented. An analysis of these measurements resulted in an empirical equation that permits prediction of this angular distribution for a variety of clouds from standard pyrheliometric measurements made at most major weather stations.

In an earlier study (Ref. 1) a large body of actinometric data was analyzed. Probability distributions of the transmittance of clouds were developed. These actinometric data were measured with two types of pyrheliometers: a wide-angle instrument that accepts radiation from the entire celestial hemisphere, and a narrow-angle instrument that tracks the sun and accepts radiation from a 5.7° full-angle heliocentric cone. The wide-angle and narrow-angle transmittances were calculated from these two measurements and from the known incident solar irradiance. The value obtained from the wide-angle pyrheliometer is the effective transmittance for a system that accepts radiation from a wide range of angles. This transmittance is also useful in estimating the light available for ordinary photography. On the other hand, the transmittance value obtained from the narrow-angle pyrheliometer applies to a system that has a suitable narrow acceptance angle. The suitability of the angle depends, unfortunately, on a number of parameters, including the cloud height and the position of the source of light being measured. If the effective narrow-angle transmittance is needed for a range of conditions, it must

be measured as a function of the scattering angle. The experiment described in this paper was designed to perform these measurements.

An instrument was developed to measure the total irradiance from the sun and the circumsolar sky for a series of angular fields of view from 1° to 32° half angle. These measurements were made and recorded automatically every ten minutes from sunrise to sunset over a six month period.

Eglin Air Force Base was selected as the site for the experiment for two reasons. The first was that this geographical area experiences the frequent occurrence of suitable cloud formations. The second was that the well-equipped Air Force weather station at the site could provide concurrent standard meteorological observational data including radar cloud height measurements.

A total of 3290 sets of measurements were made during the course of the experiment. Of these, 334 sets were obtained when there was a single overcast layer of clouds. Because of the difficulty in modeling mathematically all but this single-layer overcast data, the analysis presented here is based on these 334 data sets.

A model equation that gives reasonable agreement to the measured data is:

$$T = A + B \sin^{n}\theta$$

where T is the transmittance, θ the half angle of the field of view, and A and B parameters. These parameters were found to correlate well with the standard wide- and narrow-angle pyrheliometric transmittance measurements. These parameters, expressed in terms of T_w and T_n, which are the transmittances measured with the wide-angle and narrow-angle pyrheliometers, respectively, are:

$$A = -0.0056 + 0.89 \times T_n$$

$$B = -0.028 + 1.09 \times T_w$$

This model represents an angular scattering distribution consisting of an undeviated component plus a component which has been diffusely scattered. This should serve as an adequate model for cloud scattering profiles.

II. BACKGROUND AND PREVIOUS WORK

The optical engineer needs a fairly detailed knowledge of the transmission and scattering properties of clouds when designing a visible optical system to operate in the presence of clouds. While this subject has been treated extensively from a theoretical view point (Ref. 2), surprisingly few experimental measurements have been made by which the theories can be checked.

Haurwitz (Ref. 3) has correlated measurements of the total radiation from the sun and sky with cloud type and solar elevation angle. Unfortunately, these measurements give no information about the angular scattering distributions produced by the clouds since the measurements were made with a 2π field of view detector. Gibbons and coworkers (Refs. 4-6) have made studies of the effect of field of view on horizontal atmospheric transmission measurements. These measurements give the scattering properties of the atmosphere plus aerosols, haze, etc., but tell nothing about clouds. Arnulf and coworkers (Ref. 7) have made transmission measurements of haze and fog but unfortunately only with a detector with a narrow angle field of view. The aircraft-based measurements of Neiburger (Ref. 8) and Griggs and Marggraf (Refs. 9 and 10) of the transmission of solar radiation through clouds were again, unfortunately, made only with 2π field of view detectors.

III. INSTRUMENTATION AND EXPERIMENTAL DESIGN

A. EXPERIMENTAL DESIGN

In designing the experiment, several requirements were laid down. The first was that the experiment should run automatically with a minimum of maintenance and adjustment. This was necessary because a large number of measurements would need to be made in order to accumulate a good statistical sample.

The second requirement was that the experimental site be subject to a wide variety of cloud conditions. The panhandle region of Florida experiences the tail ends of the winter storms that sweep down across the United States from Canada and the Arctic. In the summer, cumulus clouds are prevalent due to the moisture-laden Gulf air.

The third requirement was that the experimental site be located near a well-equipped weather station. This would facilitate concurrent observations of meteorological conditions on a routine basis.

The fourth requirement was for simultaneous narrow- and wide-angle pyrheliometric measurements. This would allow for testing possible correlations of the experimental measurements with standard solar radiation measurements that are made on a routine basis at many stations around the world.

The first requirement was met in the actual design of the instrument. The second and third were met in the experimental site selection. Eglin Air Force Base near Pensacola in northwestern Florida (latitude 30°29'N, longitude 86°31'W) has a well-equipped weather station staffed by personnel of Detachment 10 of the 6th Weather Wing, United States Air Force. In addition to the standard meteorological instrumentation, this station also has a cloud

height radar, AN/TPQ-11, operating routinely. The fourth requirement was met by the inclusion of standard narrow- and wide-angle pyrheliometers[1] in the experimental setup.

B. INSTRUMENTATION

The basic components of the instrument designed to measure the angular scattering profiles of clouds, hereafter called the cloud scattering instrument, are a lens, a series of field stops, an integrating sphere, and a detector. The arrangement is shown in Figure 1. The lens is a Nikkor 21mm focal length, f/4 35mm camera lens. The field stops are thirteen holes drilled in a rotating disc plus an opaque position. The hole sizes correspond to field of view ranging from 0.95° to 32.2° half angle. The integrating sphere is made from two 9-inch diameter plastic hemispheres with holes drilled at their "poles" for the entering and exiting light. The sphere is painted on the inside with 3M "White Velvet Coating", which is a 50-50 mixture of titanium dioxide and silicon dioxide. The detector is prevented from seeing direct radiation by a spider-mounted baffle on the optic axis 1.5 inches from the face of the detector. The detector is an RCA 7764 multiplier phototube with an S-11 response. This tube has its maximum response between 3900Å and 4900Å, and 50% sensitivity points at 3500 and 5700Å (Ref. 11).

The instrument is enclosed in a weather-tight box with an outer window of glass with a thin layer of evaporated chromium to act as a neutral density filter and heat reflector. Mounted on the same base plate and bore sighted

[1] These instruments were loaned to The Aerospace Corporation by the Army Electronics Proving Ground at Fort Huachuca, Arizona, through the efforts of Capt. L. Johnson of Detachment 50, 6th Weather Wing, Space and Missile Systems Organization, Air Force Systems Command, Los Angeles, California

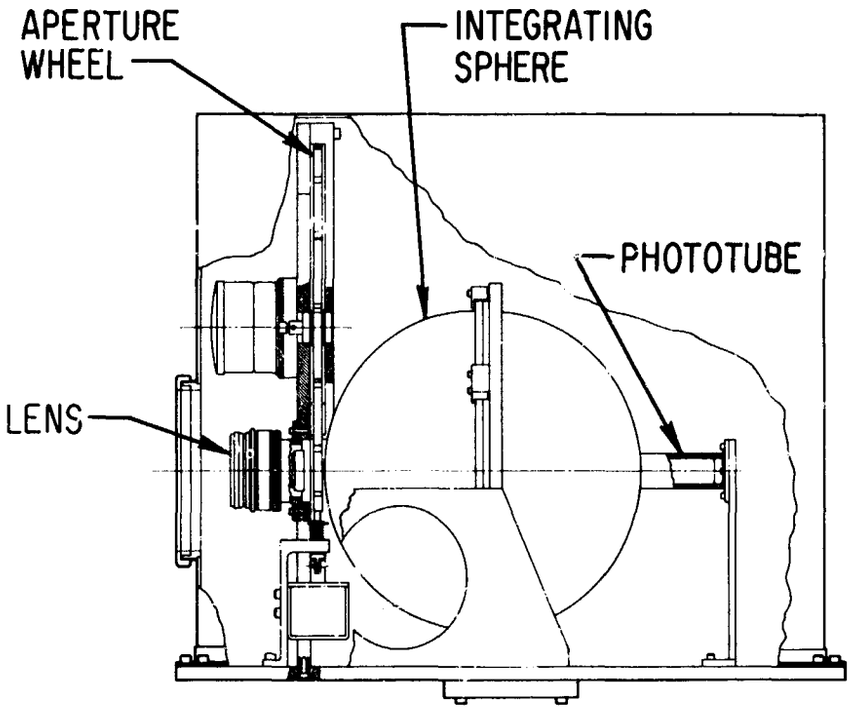

Figure 1. Optical Diagram

with the cloud scattering instrument is an Epply narrow-angle (2.85° half angle field of view), normal incidence pyrheliometer. The pyrheliometer has a visual indicator of correct solar pointing that can be used when the sun is shining to adjust the alignment of the two instruments during operation.

The instrument and the narrow-angle pyrheliometer are mounted on a conventional astronomical telescope clock drive whose polar axis was carefully aligned to true north. An appropriate declination adjustment of the instruments permitted correct tracking of the sun with the sun centered in the fields of view of the apertures. Electrical and signal connections are made through a set of slip rings mounted on the polar axle to prevent wind up of the cabling by the rotation of the drive.

The instrument was placed on a wooden platform on the roof of a hangar at Eglin Air Force Base approximately 50 feet above the ground. Figures 2 and 3 show the instrument in place. An Eppley wide-angle (2π field of view), horizontal incidence pyrheliometer was placed in an unshaded location on the roof of a small penthouse near the instrument.

The power and signal cabling was run approximately 200 feet to the Weather Operations room on the floor of the hangar where the recording electronics were housed. Because of the long cable run, preamplifiers were included in the weather-proof box.

The recording electronics consisted of a Hewlett-Packard Model 3440A Digital Voltmeter with a Model 3443A High Gain/Auto Range plug-in unit, a Hewlett-Packard Model 562AR-J74 Digital Recorder, a Parabam Digital Clock/Calendar, and additional automatic sequencing electronics built at The Aerospace Corporation.

The operation of the experiment was as follows. A 24-hour timer turned the electronics on before sunrise and off after sunset. A set of data s taken automatically every 10 min during this time. The instrument

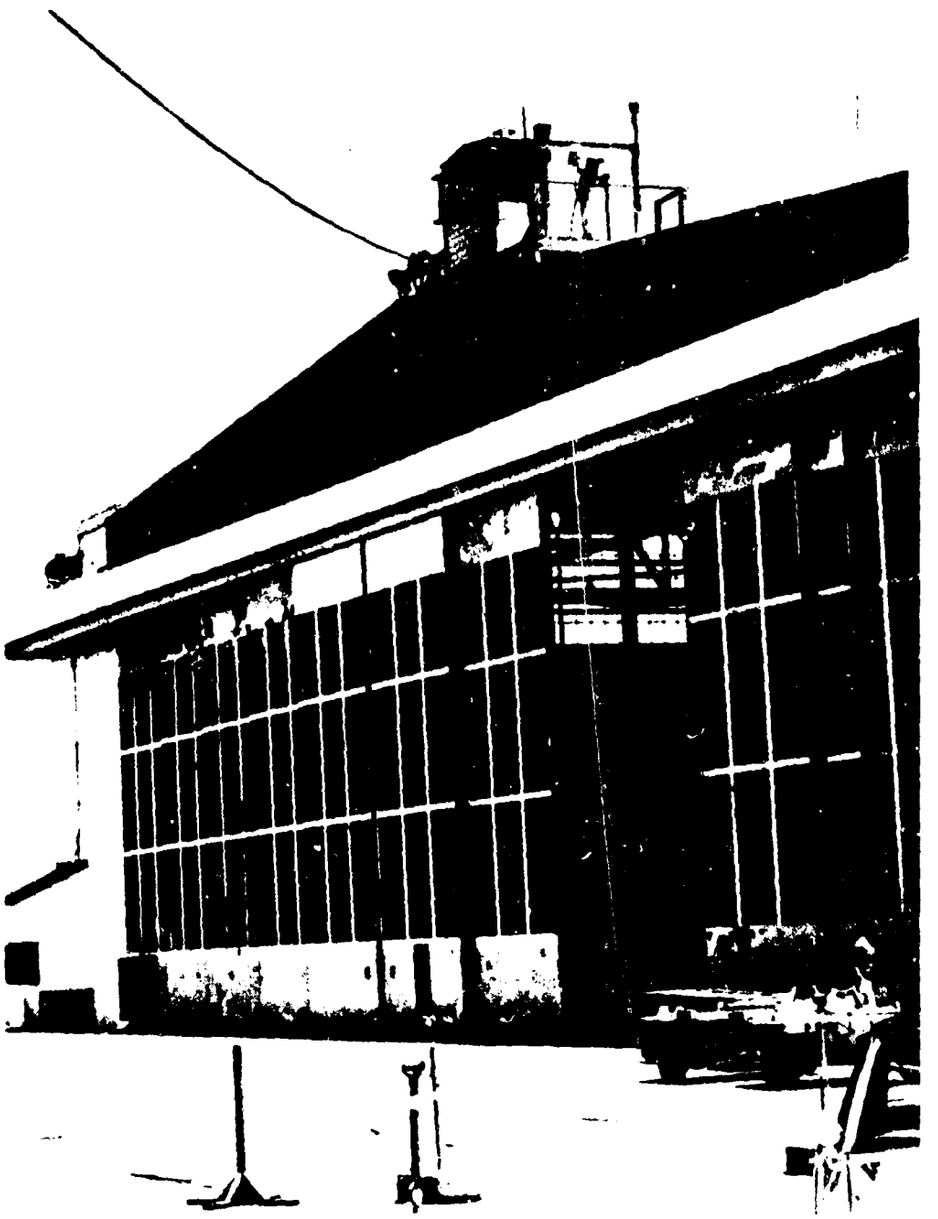

Figure 2. Photograph of the Instrument as Seen From the Ground

Figure 3. Photograph of Instrument as Seen From the Roof

sequenced through the thirteen apertures from smallest to largest, stopping 1-2 seconds at each aperture to allow recording of the signal. After sequencing through the thirteen apertures, the instrument turned itself off at the opaque position. A zero (opaque) reading was taken at the start and end of each sequence. After cycling through the apertures, the instrument recorded the signals from the two pyrheliometers. Thermistors located in the cloud instrument and each of the pyrheliometers were also sampled. Finally, the minute, hour, and day number were recorded from the digital clock/calendar. The entire cycle took about a minute, after which the electronics went into standby until ten minutes elapsed.

The pyrheliometric measurements were made with two standard Eppley pyrheliometers, a 50-junction hemispheric pyrheliometer, and a Model 15 normal-incidence pyrheliometer (Ref. 12). The cloud height radar in operation at Eglin Air Force Base was a Model AN/TPQ-11 Radar Cloud Detecting Set operating in the K_A frequency band (33-36 GHz) (Ref. 13). The facsimile chart recordings from this instrument were provided to The Aerospace Corporation personnel who made the interpretations. These interpretations were made by combining the standard observations of the clouds and the indicated clouds on the charts. This was necessitated by the inability of the AN/TPQ-11 to detect all clouds. Kantor (Ref. 14) has analyzed the detection capabilities of the AN/TPQ-11 radar and found that only 62% of visually-observed overcast clouds were detected by the radar.

Standard meteorological observational data were supplied by the personnel at Eglin Air Force Base on WBAN Form 10 "Surface Weather Observations." The WBAN Form 10 includes the following data used in this experiment: time, sky condition, horizontal visibility, temperature and dew point, total sky cover, remarks, and supplemental coded data. Observations were made hourly except when rapidly changing conditions warranted more frequent observations. The supplemental coded data

included the synoptic code observations of low, middle, and high clouds ($1C_LC_MC_H$) (Ref. 15). These were recorded every three hours. These synoptic measurements were used to identify the clouds present during our measurements. Identifications between the synoptic observations were made by interpolating between the bracketing observations using the remarks recorded by the observer as to advancing or receding clouds.

C. CALIBRATION

The calibration of the cloud scattering instrument entailed several steps. All the measurements were made in a darkroom using a small but very bright tungsten coil lamp mounted in the same horizontal plane as the cloud scattering instrument and about twenty feet away. A slight adjustment in the focus of the lens of the instrument was made to correct for the non parallelism of the light from twenty feet.

The normalization factors between the apertures were determined by measuring the on-axis signal for each aperture and normalizing to the smallest aperture (1^o). These normalization factors are listed in Table 1. The effective angular field of view of each aperture was determined as follows. With no limiting aperture, the intensity is given by a $\cos^4\theta$ angular distribution.[2] The signal was measured at a number of angles on both sides of the optic axis (in a horizontal plane only). The two points at which the signal dropped to 50% of the above-mentioned $\cos^4\theta$ value were averaged to give the effective field of view of a given aperture. The results of these measurements are given in Table 2. The areas under these curves of angular response were measured with a planimeter to determine the solid angle factor for each aperture. These solid angle factors are given in Table 3.

[2] The $\cos^4\theta$ represents the fall off of intensity of off-axis rays due to geometric factors. See, for example: Jenkins and White, Fundamentals of Optics, Chapter 7.

Table 1. Aperture Normalization Factors

Aperture	Normalization Factor
1	(≡1.0000)
2.5	0.9882
5	0.9824
7	0.9824
10	0.9719
12	0.9644
14	0.9516
16	0.9143
18	0.8947
22	0.8330
26	0.8029
30	0.7928
32	0.7966

Table 2. Effective Fields of View

Aperture	Effective Field of View (Half Angle)
1	0.9583°
2.5	2.400°
5	4.858°
7	7.171°
10	9.763°
12	12.076°
14	14.290°
16	16.198°
18	18.156°
22	21.882°
26	25.882°
30	30.042°
32	32.170°

Table 3. Solid Angle Factors

Aperture	Solid Angle Factor
1	0.0002688
2.5	0.0017617
5	0.0071867
7	0.015631
10	0.028955
12	0.044267
14	0.061882
16	0.079400
18	0.099587
22	0.14410
26	0.20062
30	0.26868
32	0.30705

The conversion-calibration factor in langleys/min/volt[3] for each of the pyrheliometers is given by the Eppley Company with their instruments. An additional calibration factor required is the gain of the preamplifiers that take the low-level pyrheliometer output and amplify it prior to its being transmitted down the long signal cable. It was impossible to calibrate the entire pyrheliometer-preamplifier-signal cable assembly as installed in Florida. An indirect method of calibration had to be applied.

Several crystal-clear days with very high reported horizontal visibility occurred in the early period of the experiment. The calculated transmittance of a Rayleigh atmosphere in the spectral region passed by the glass bulb of the pyrheliometers is 0.904 and the calculated transmittance of a turbid atmosphere is 0.718.[4] Since the atmospheric conditions on these crystal-clear days seemed to be clearer than those described by Elterman for his "turbid" atmosphere, the simple Rayleigh atmospheric transmittance of 0.90 was adopted for the pyrheliometric readings on these days. With the use of this value of the transmittance, the calibration factors of the pyrheliometers were calculated. The absolute accuracy of the pyrheliometric measurements does not affect the shapes of the angular scattering profiles that are more significant to this study than the absolute magnitudes.

---

[3] A langley is 1.0 cal/cm^2.

[4] The calculated transmissions are based on Elterman's atmospheric attenuation model as given in Handbook of Geophysics and Space Environments, U. S. Air Force Cambridge Research Laboratories. New York: McGraw-Hill Book Co , Inc., 1965, Chapter 7. The spectral range was considered to be that passed by the glass window or envelope of the pyrheliometers; namely 0.35 to 2.5 microns. The sun with a spectral distribution as given in Chapter 16 of the Handbook was used for the radiation source.

IV. EXPERIMENTAL OPERATION AND DATA SAMPLE

A. PERIOD OF EXPERIMENT

The experiment was operated between 9 February and 18 October 1968. Because of equipment malfunctions, data were obtained only for the periods 9 February through 3 April, 5 April through 9 April, 17 April through 22 May, 12 June through 21 July, 28 August through 4 October, and 16 October through 18 October. The data for 15 May through 22 May were lost in the mails. The narrow-angle pyrheliometer was inoperative for the period 12 June through 21 July. The data for the period 28 August to the end of the experiment are considered unreliable because of a belatedly discovered possible misfocus and f/stop change. Reliable, complete data are available, therefore, only for 88 days between 9 February and 14 May. In addition, incomplete data (narrow-angle pyrheliometer inoperative) are available for the 40-day period between 12 June and 21 July.

B. DATA SAMPLE

During the 88-day period for which complete data are available, a total of 3296 measurements were made during times when the sun was higher than 35° above the horizon. Of these 3296 measurements, 530 were made during completely clear skies (0/10's cloud cover) and 1200 during completely overcast skies (10/10's cloud cover). The 1566 measurements made during periods of broken or scattered clouds were not used for further analysis because of the uncertain location of holes in the clouds with respect to the sun's position. In addition, measurements of overcast clouds made when more than one layer of clouds was reported were also not used for further analysis. This was because of uncertainties about breaks in the individual layers. This left a sample of 530 measurements during completely clear skies and 398 measurements made during single-layer, completely overcast skies. Of the 398 overcast measurements, 64 were discarded because of various problems with the data.

Table 4 gives a breakdown of the 3296 measurements by the amount of cloud cover. Table 5 gives a breakdown of the 1200 overcast measurements by the number of cloud layers reported. Table 6 further breaks down the single-layer overcast measurements into reported cloud types. This table gives the breakdown of the measurements upon which the analysis was based.

Table 4. Number of Measurements Made by Amount of Cloud Cover (Solar Elevation Angle $\geq 35^{\circ}$)

Cloud Cover	Number of Measurements
0/10	530
1/10	236
2/10	152
3/10	142
4/10	189
5/10	109
6/10	112
7/10	215
8/10	214
9/10	168
10/10	1200
Broken (6/10 to 9/10)	7
Scattered (1/10 to 5/10)	16
Unknown	6
Total	3296

Table 5. Number of Measurements of 10/10's Cloud Cover by Number of Cloud Layers Reported

Number of Cloud Layers	Number of Measurements
1	398
2	486
3	249
≥4	67
Total	1200

Table 6. Number of Complete Measurements of Single-Layer 10/10's Cloud Cover by Cloud Type

Cloud Type	Name	No. of Measurements
Low clouds		
$C_L = 3$	Cumulonimbus	3
$C_L = 4$	Stratocumulus cumulogenitus	5
$C_L = 5$	Stratocumulus	34
$C_L = 6$	Stratus	127
Middle clouds		
$C_M = 1$	Altostratus	5
$C_M = 3$	Altocumulus translucidus	5
$C_M = 7$	Altocumulus opacus	17
High clouds		
$C_H = 1$	Cirrus fibratus	5
$C_H = 7$	Cirrostratus	133
Incomplete data or unknown cloud type		64

V. DATA REDUCTION

The first stage in the data reduction scheme was the laborious manual transcription of the data from the digital printer tapes to computer coding sheets. This was done by the computress staff in the Space Physics Laboratory at The Aerospace Corporation.

Three cards were used to encode all the data for each observation. The data included for each observation were the following: day, time, wide-angle pyrheliometer reading, narrow-angle pyrheliometer reading, photo-tube initial and final zero readings, the thirteen aperture readings, the thermistor readings of the two pyrheliometers and the phototube, an abbreviated description of the weather and obscurations to vision, the total cloud cover, the horizontal visibility, the air temperature and dew point, and a description of up to four layers of clouds. This description included the coverage of the individual layer, the type of cloud, and the base and top of the layer.

A computer program was written (by R. T. H.) which took these three cards for each observation and computed the mean relative radiance and irradiance, the wide- and narrow-angle transmittances, the relative humidity, and the solar elevation angle. All these data were printed by the computer on one page together with verbal descriptions of the weather and clouds. Plots were made on 35-mm film of the mean relative radiance and irradiance as a function of the field of view. An example of a page of computed data is given in Figure 4.

DAY 99 TIME 850 SOLAR ELEVATION ANGLE 42.70 DEGREES TOTAL CLOUD COVER 10
TEMPERATURE 68 DEGREES F., RELATIVE HUMIDITY 90 %, HORIZONTAL VISIBILITY 2.5 MILES
PPT(WITHOUT ANGULAR FACTOR) 12.85%, PPT 20.12%, PPN, .24%, ZERO 2.800E-04, ZERO VARIANCE 4.000E-05
WEATHER AND OBSTRUCTIONS TO VISION
PARTIALLY OBSCURED SKY

OBSTRUCTION TO VISION - FOG

CLOUD LAYER 1
10 TENTHS COVER OF LOW CLOUD TYPE 6
WITH ITS BASE AT 400 FEET AND ITS TOP AT 2000 FEET.
NO OTHER LAYERS

THETA, DEGREES	RELATIVE IRRADIANCE	RELATIVE RADIANCE
32.1700	.07552	2.4596E-01
30.0420	.06705	2.4955E-01
25.8820	.05066	2.5254E-01
21.8820	.03593	2.4934E-01
18.1560	.02417	2.4268E-01
16.1980	.01900	2.3930E-01
14.2900	.01471	2.3771E-01
12.0760	.01042	2.3529E-01
9.7630	.00733	2.5300E-01
7.1710	.00432	2.7619E-01
4.8580	.00196	2.7265E-01
2.4000	.00047	2.6678E-01
.9583	.00007	2.6042E-01

Figure 4. Sample Output Data Sheet

The relationships used to compute the various output quantities[5] are the following:

$$\text{IRRAD(I)} = [\text{READING(I)} - \text{ZERO}] \times \text{NFAC(I)} \tag{1}$$

$$\text{RAD(I)} = \text{IRRAD(I)}/\text{SAF(I)} \tag{2}$$

$$\text{RELHUM} = [\text{VP(DEWPT)}/\text{VP(TEMP)}] \times 100 \tag{3}$$

$$\sin \gamma = \sin \delta \sin \phi + \cos \delta \cos \Omega \cos \phi \text{ (Ref. 16)} \tag{4}$$

$$\Omega = \text{TIME} - 11.76722 \tag{5}$$

$$\cos \beta = \sin \gamma \left[\cos \epsilon + \sin \epsilon \cos A \tan \phi\right] - \text{(Ref. 16)} \tag{6}$$

$$\sin \delta \sin \epsilon \cos A \sec \phi + \cos \delta \sin \Omega \sin \epsilon \sin A$$

$$I_o = 2.000/R_v^2 \text{ (Ref. 16)} \tag{7}$$

$$T_{wW} = [WA/I_o] \tag{8}$$

$$T_w = T_{wW}/\cos \beta^6 \text{ (Ref. 16)} \tag{9}$$

$$T_n = [NA/I_o] \tag{10}$$

The definitions of the quantities in these equations are:

IRRAD(I) = mean relative irradiance for aperture I

ZERO = average of initial and final zero readings

READING(I) = reading for aperture I

NFAC(I) = normalization factor for aperture I

RAD(I) = mean relative radiance for aperture I

SAF(I) = solid angle factor for aperture I

RELHUM = relative humidity

VP(I) = vapor pressure of water at temperature I

DEWPT = dew point temperature

---

[5]Not all these quantities were actually used in the final analysis. Printouts of the complete output data are available from the author.

[6]It should be noted that $\cos \beta = \sin \gamma$ for a horizontal plane, and Equation 9 would take its usual form $T_w = T_{wW}/\sin \gamma$.

TEMP = air temperature

γ = solar elevation angle

δ = solar declination angle

ϕ = latitude ($30^{o}29'$N for Eglin AFB)

Ω = hour angle (11.76722 is the local Central Standard Time of true solar noon at Eglin AFB)

β = angle between the solar elevation angle, γ, and the normal to an arbitrarily inclined plane

ϵ = angle between a horizontal plane and an arbitrarily inclined plane

A = azimuth of the vertical plane containing the normal to an arbitrarily inclined plane

I_o = amount of solar radiation incident at the top of the atmosphere (2.000 langleys per minute is the solar constant used)

R_v = radius vector of the sun (earth-sun distance)

T_{wW} = wide-angle transmittance of the sun's radiation not taking into account the solar elevation angle

T_w = narrow-angle transmittance

WA = wide-angle pyrheliometer calibrated reading

NA = narrow-angle pyrheliometer calibrated reading

The quantities β and ϵ above were necessitated by a small tilt ($\sim 3^{o}$WNW) of the wide-angle, horizontal incidence pyrheliometer which occurred shortly after its installation. The correction resulted in approximately a 5% change in the wide-angle pyrheliometer readings.

VI. ANALYSIS AND RESULTS

A. ANALYSIS

The goal of the experiment was the development of a realistic model of the angular scattering profiles of clouds for use in designing visible-light optical systems. It was hoped that the observed scattering profiles could be correlated with some routinely observed meteorological quantity or quantities so that system performances could be predicted from readily available meteorological data.

Various correlations and relationships were tried. The most obvious is a correlation between the irradiance measurements and the cloud type. This correlation was tried and failed. This failure is probably due to the great variability in cloud characteristics within a cloud type. The same cloud can exist over a wide range of thicknesses and opacities.

The failure of this obvious correlation prompted a search for some other way of describing the scattering profiles, such as a combination of the measures of the direct and diffuse solar radiation. This description should be reasonable in light of the observation that on a clear day the sun's radiation is virtually entirely direct and that on a heavily overcast day the sun's radiation which penetrates to the earth is entirely diffuse. All other cases should be some combination of these two extremes. The intermediate cases can be described by a bright spot at the position of the sun surrounded by a diffusely scattering region.

The results as derived by the computer analysis are in terms of relative irradiances. A more useful quantity is the transmittance. Since there was no way to derive absolute transmittances from the relative irradiances an alternative was to derive the transmittances relative to a clear sky. The transmittances could be determined from the relative

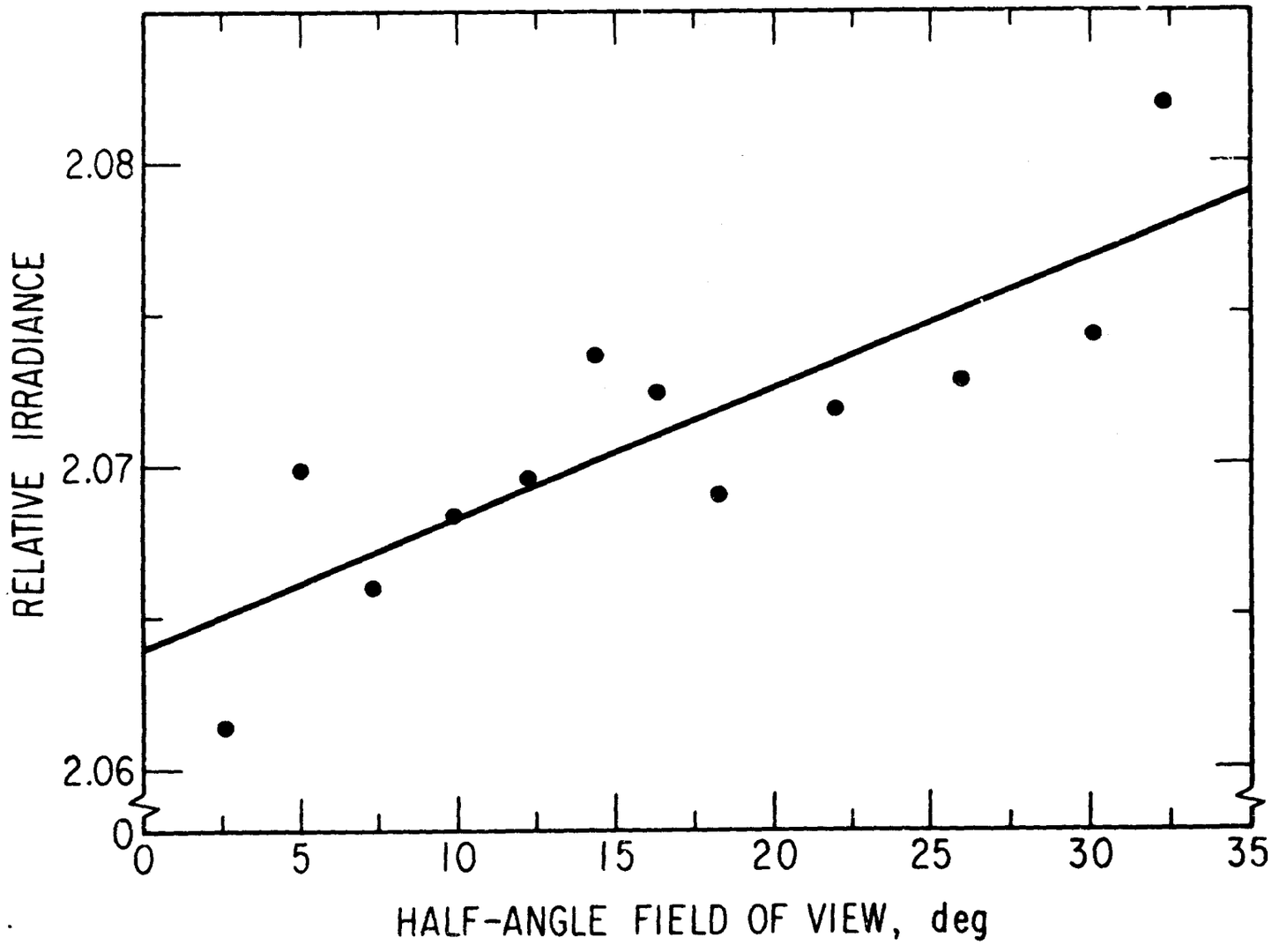

Figure 5. Relative Irradiance Plot for 1205 Hours, 1 March 1968

Table 7. Relative Irradiance and Least-Squares Values for Clear Sky Case

θ	Relative Irradiance	Least-Squares Value
0.9583	---	2.06447
2.400	2.06147	2.06509
4.858	2.06995	2.06613
7.171	2.06613	2.06712
9.763	2.06845	2.06822
12.076	2.06969	2.06920
14.290	2.07364	2.07014
16.198	2.07244	2.07096
18.156	2.06909	2.07179
21.882	2.07186	2.07337
25.882	2.07277	2.07508
30.042	2.07434	2.07685
32.170	2.08186	2.07775

$$(\text{Relative Irradiance})_{\text{clear sky}} = 2.064064 + 0.0004255\theta$$

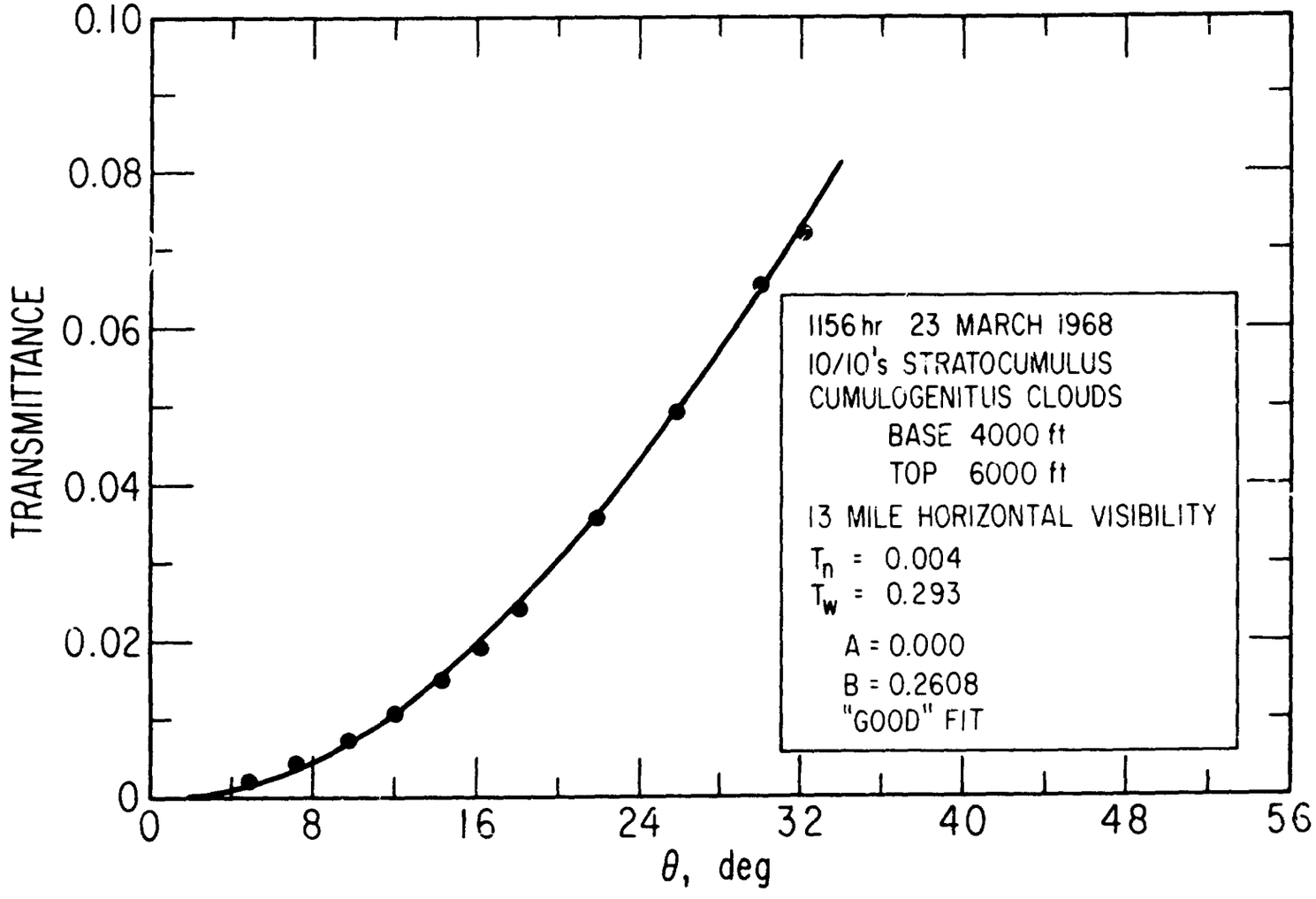

Figure 6a. Sample Plot Showing Example of Quality of Fit

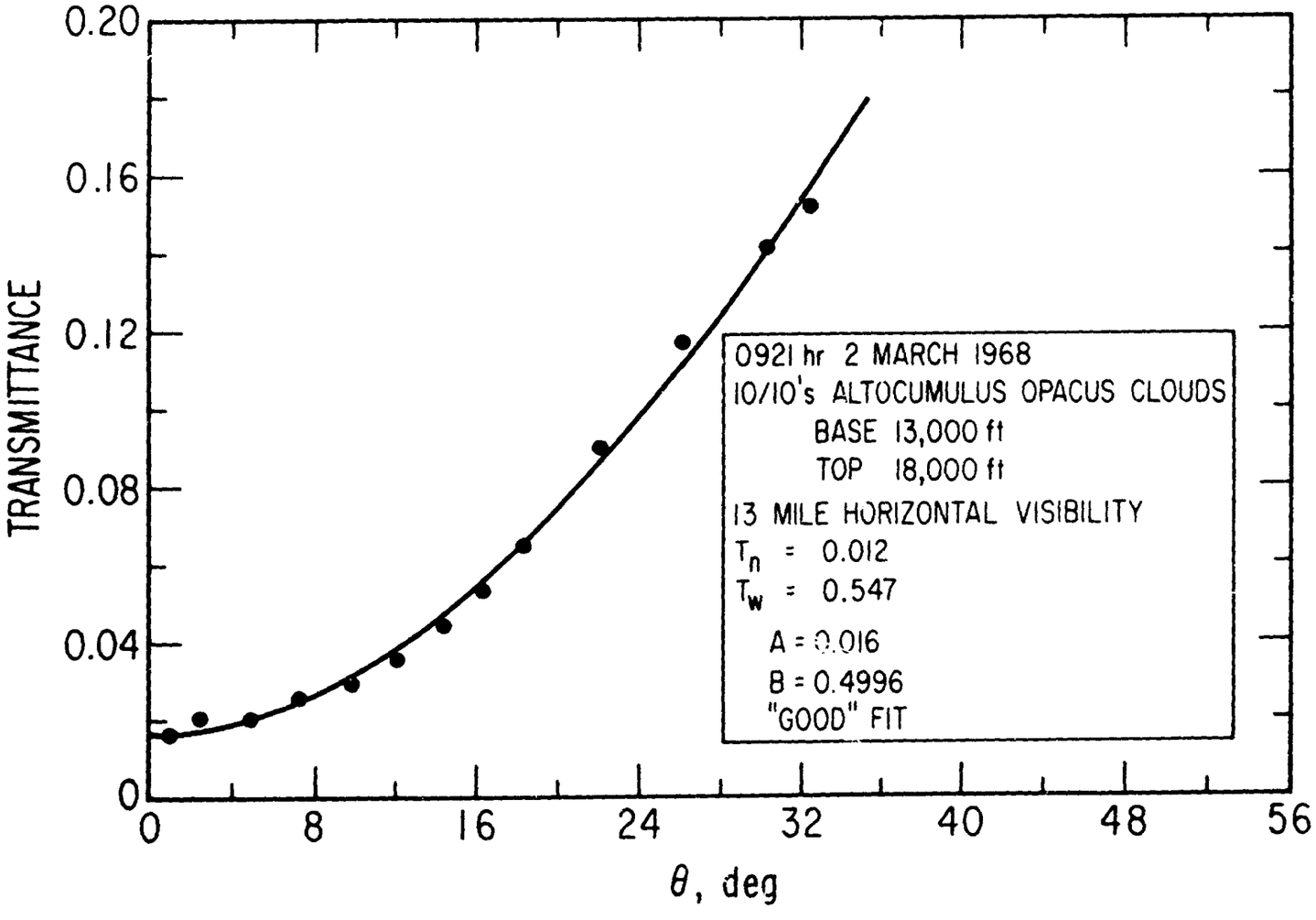

Figure 6b. Sample Plot Showing Example of Quality of Fit

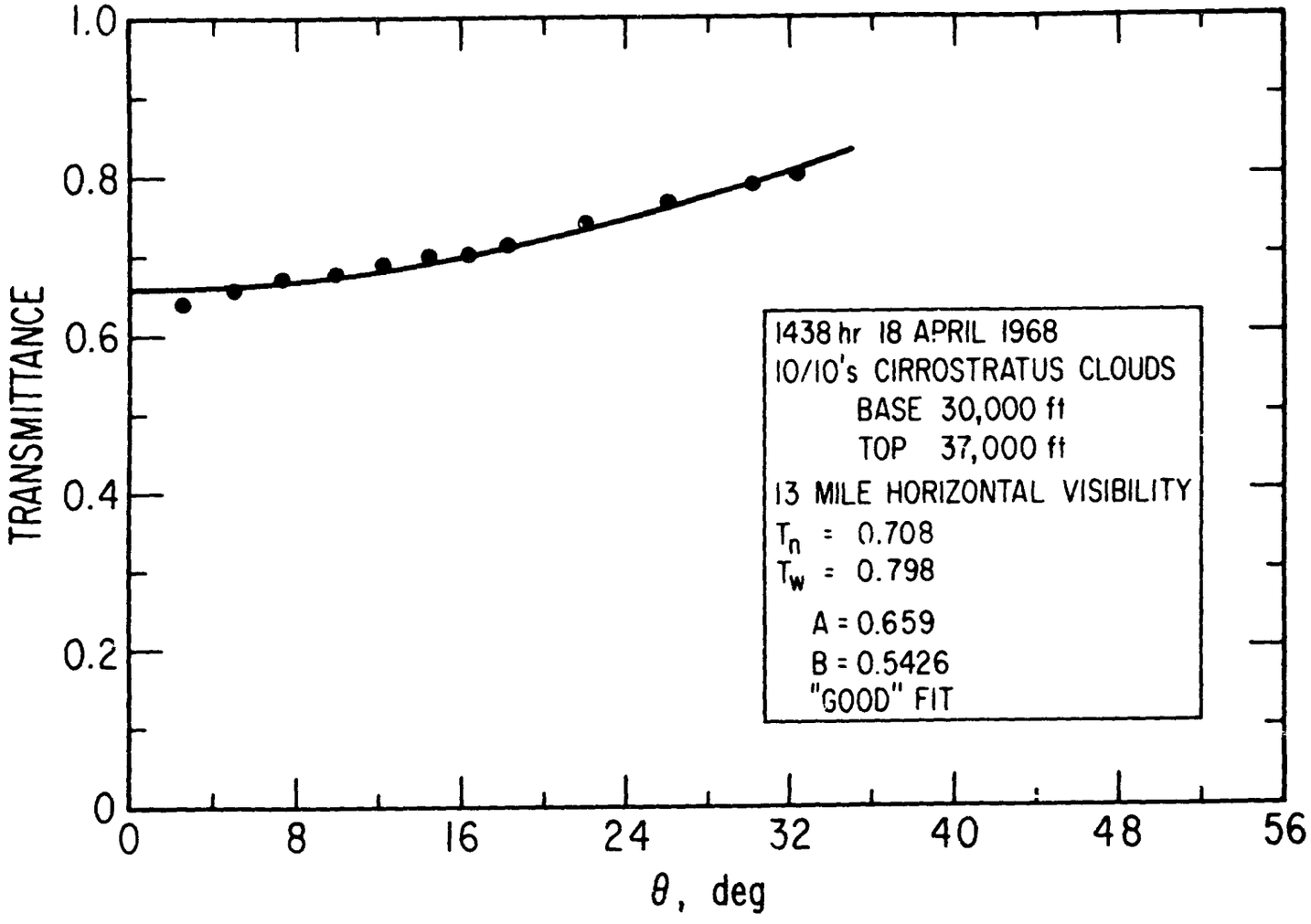

Figure 6c. Sample Plot Showing Example of Quality of Fit

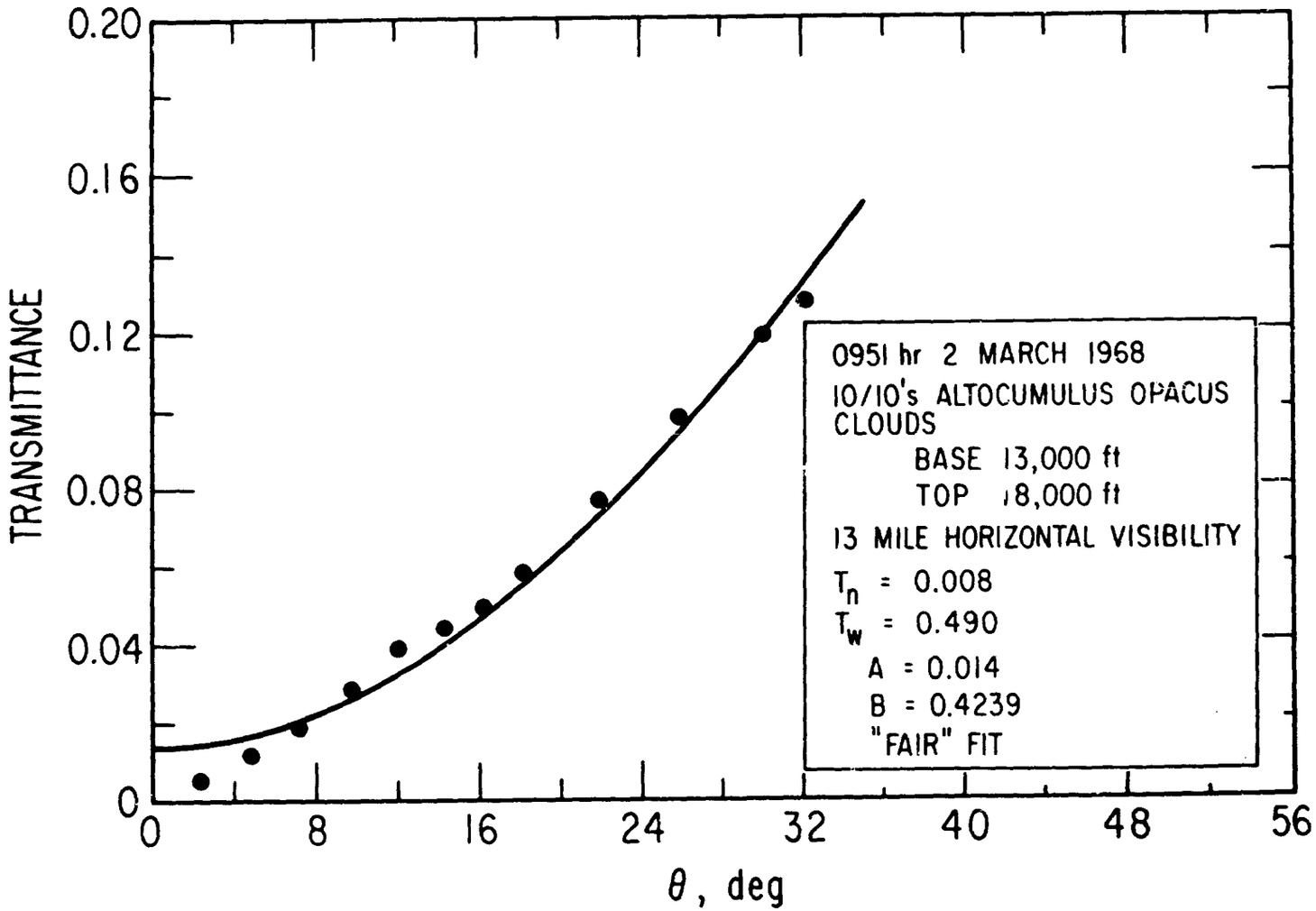

Figure 6d. Sample Plot Showing Example of Quality of Fit

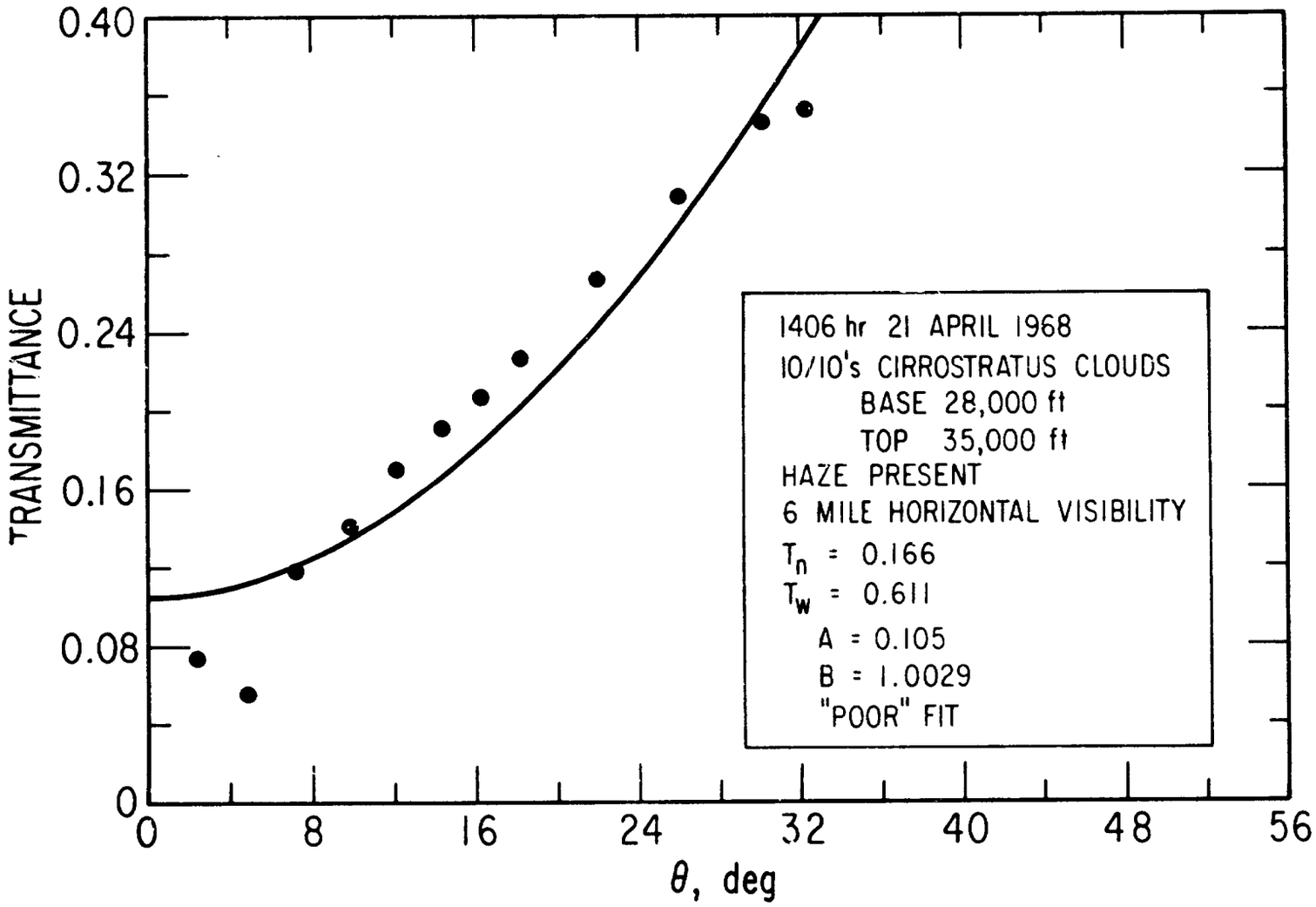

Figure 6e. Sample Plot Showing Example of Quality of Fit

With the coefficients A and B available as descriptors of the transmittance profiles, correlations of these coefficients with routinely measured actinometric quantities could be tested. The four combinations of A and B with T_w and T_n were tested for possible correlations. Separate tests were made for "good", "fair", "poor", "good + fair", and all data. Some of these plots are shown in Figures 7-10.

Looking at Figure 7 there appears to be a linear correlation with an origin intercept between T_n and A. This is reasonable in view of the fact that both are measures of the direct sunlight. A linear correlation with origin intercept between T_w and B is again indicated in Figure 8 although the scatter is fairly great at large values of T_w. This correlation is also reasonable in view of the fact that both quantities are measures of the diffuse radiation.

Figure 9 shows no simple correlation between T_n and B as would be expected. Figure 10 illustrates a more complex situation. A linear correlation seems to exist between T_w and A but with a non-zero intercept. It would seem that a threshold value of T_w must be exceeded before A has a nonzero value. This is reasonable from the observation that the sun can be seen through the clouds only for a range of transparency of the clouds. For more opaque clouds no direct sunlight can be seen.

Linear least-squares fits of these data and their correlation coefficients were calculated to quantify these visual correlations. The "poor" data were omitted from these calculations. The calculations for T_w versus B and T_n versus A are straightforward. The calculation of T_w versus A requires that the threshold point be determined first. The threshold point was found by using only those points in the least-squares

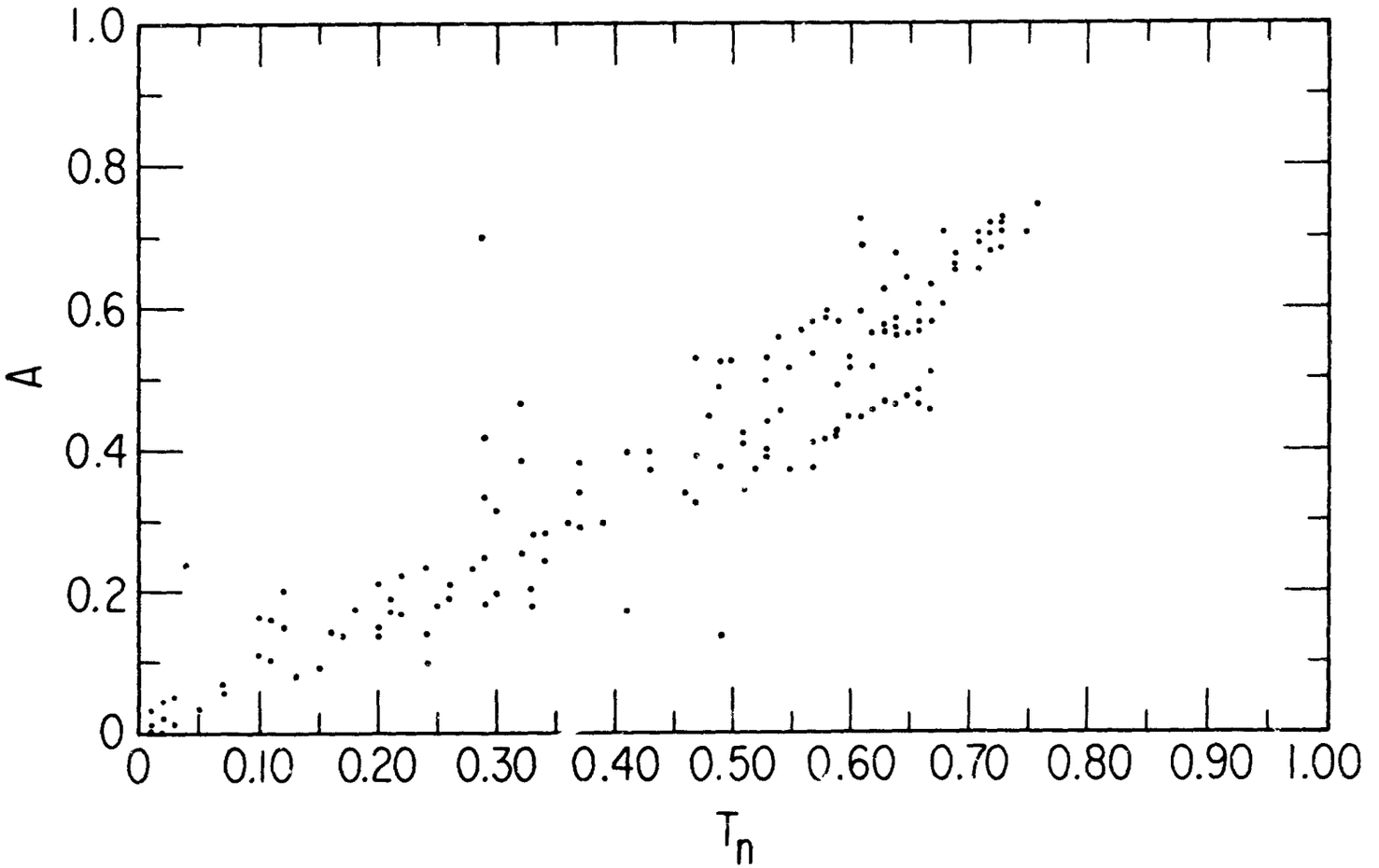

Figure 7. Plot of T_n vs A

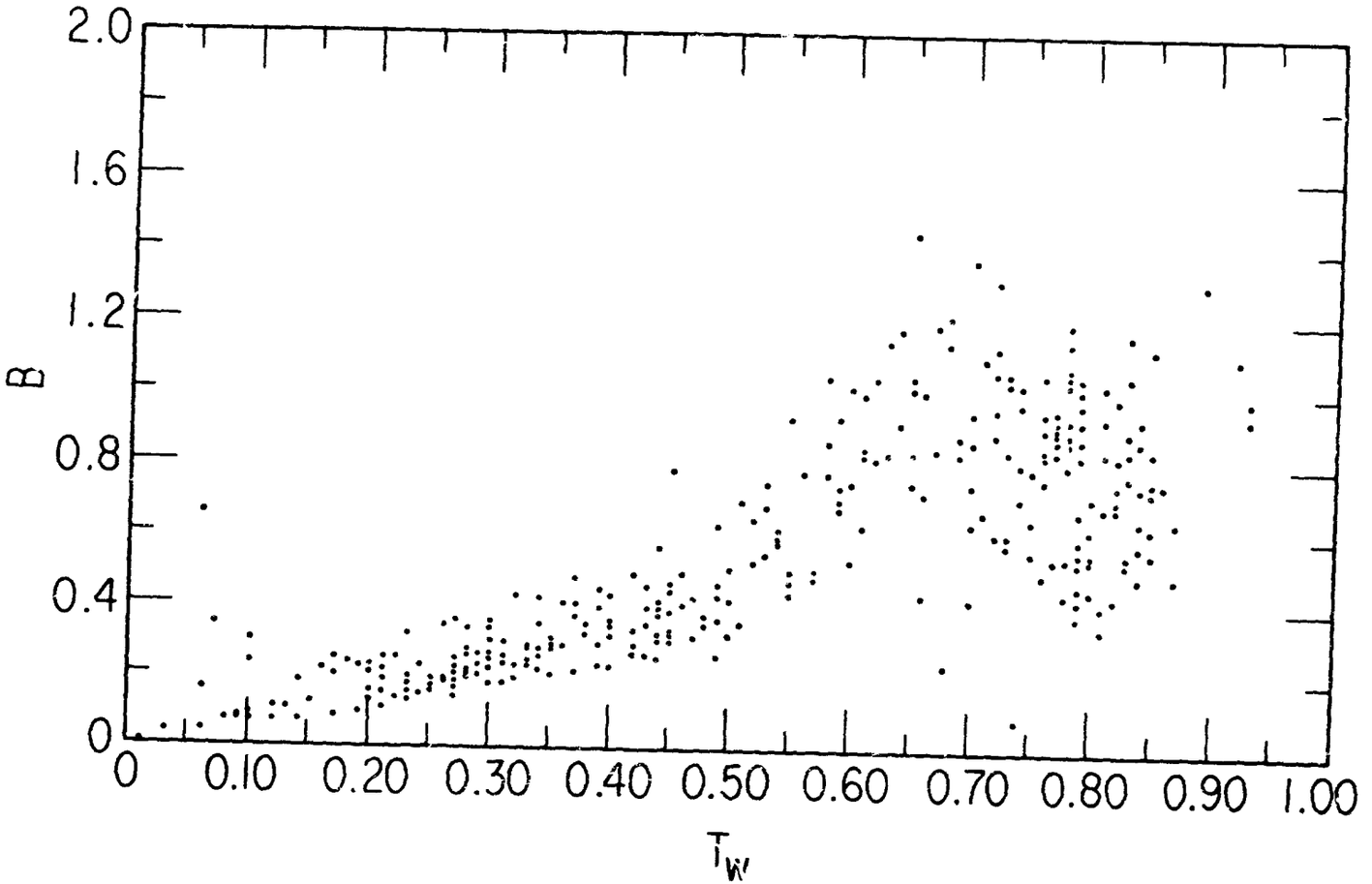

Figure 8. Plot of T_w vs B

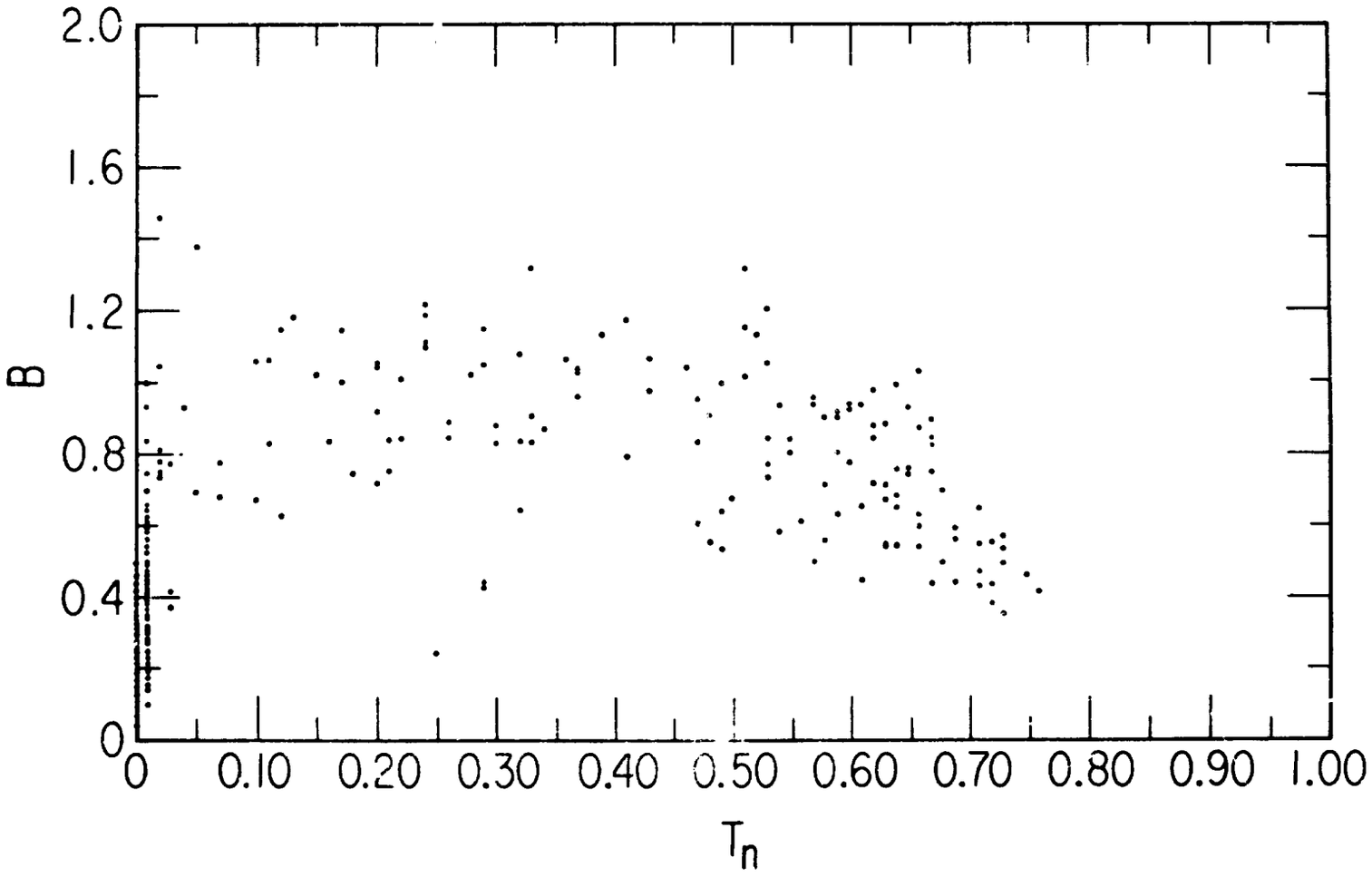

Figure 9. Plot of T_n vs B

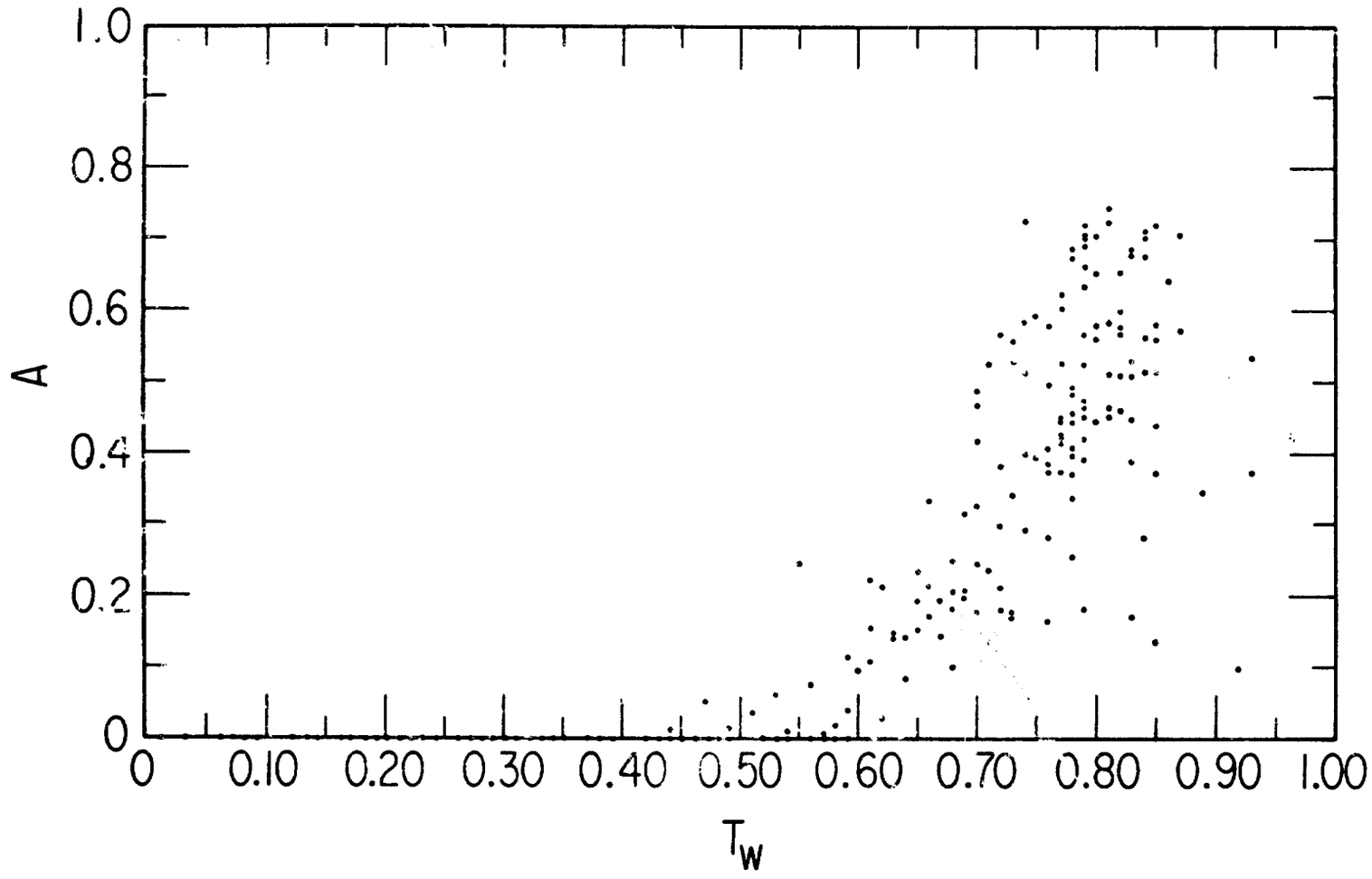

Figure 10. Plot of T_w vs A

calculations whose T_w coordinate was above some arbitrary value. The threshold point was defined when the T_w cutoff most nearly equalled the T_w-axis intercept. The threshold determined by this method was 0.54. The results of the linear least-squares calculations are plotted in Figures 11-13 and tabulated in Table 8.

An additional correlation between T_w and T_n was tested. These data are shown in Figure 14. The results are qualitatively similar to those for the correlation between T_w and A. The least-squares fit with a T_w threshold of 0.54 gave the straight line shown in Figure 14 and the results tabulated in Table 8.

B. RESULTS

In light of the good correlation between T_n and A and between T_w and B, it would appear that a reasonable model of the angular scattering characteristics of clouds has been found which can be quantitatively calculated from two routine meteorological observations. Combining the results tabulated in Table 8 with Equation 11 results in the following formula for the visible light angular transmittance of a cloud relative to that of the clear sky as a function of the narrow- and wide-angle pyrheliometric transmittance:

$$T = -0.0056 + 0.89 \times T_n + [-0.028 + 1.09 \times T_w] \times \sin^2\theta \quad (12)$$

The formula is valid at least for $\theta \leq 35^\circ$. For larger values of θ an extrapolation of unknown accuracy is assumed.

How well this model will predict the angular transmittance profiles is shown in Figures 15a-e. The data are the same as used in Figures 6a-e. The lines in the figures are calculated from Equation 12; the points are the observed data. The agreement of the calculated lines

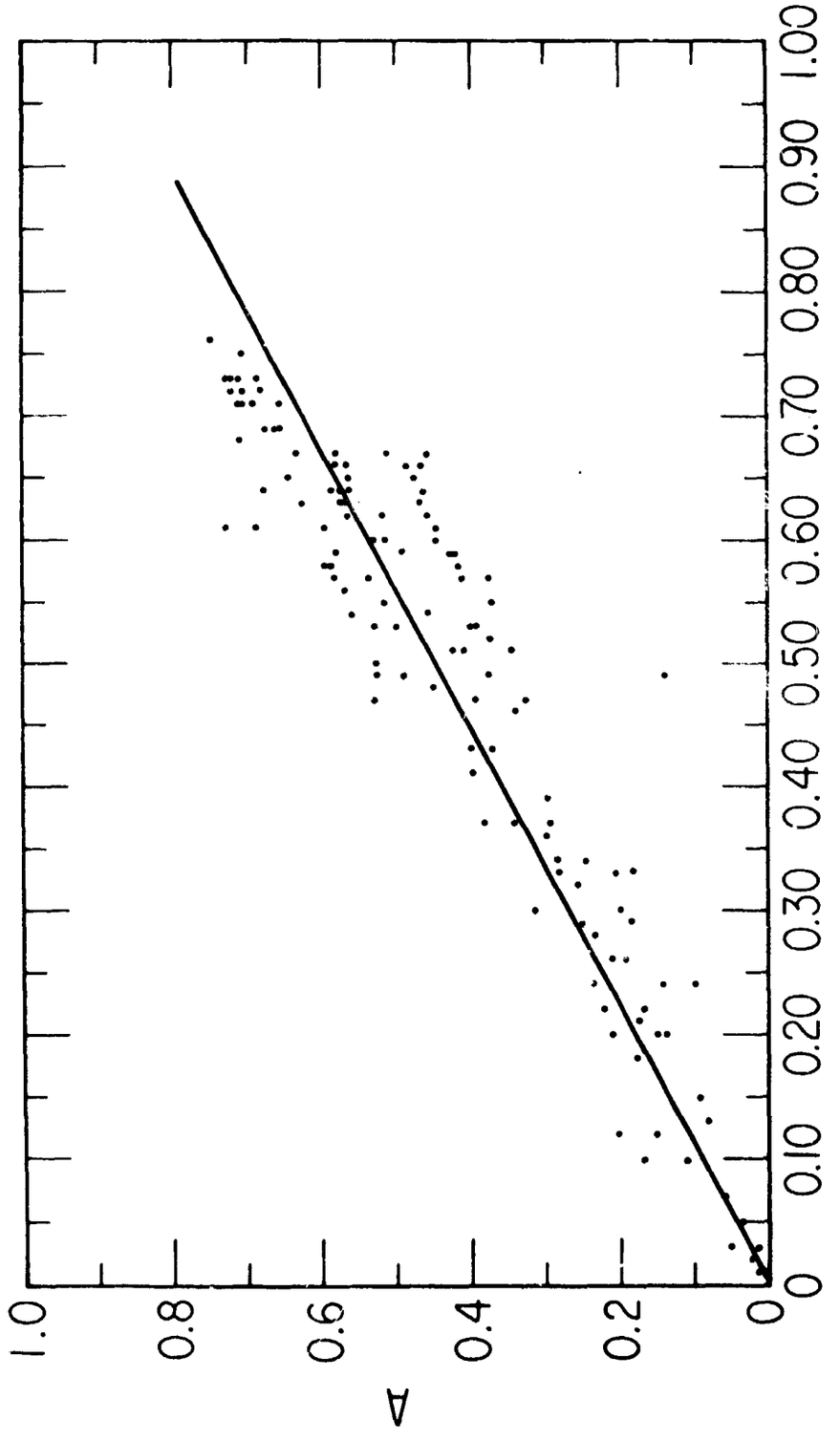

Figure 11. Plot of T_n vs A Showing Linear Least-Squares Fitted Line

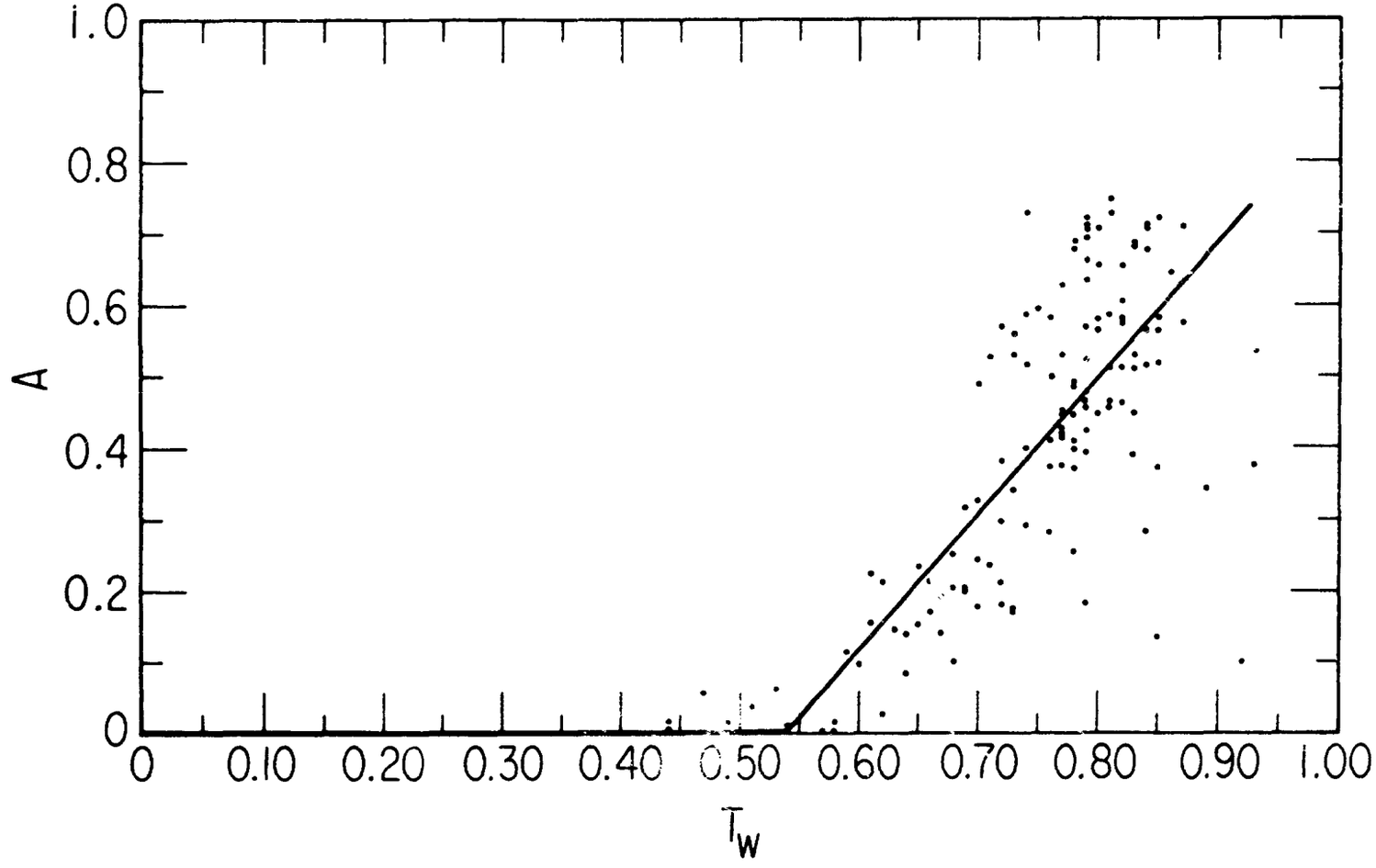

Figure 12. Plot of T_w vs A Showing Linear Least-Squares Fitted Line

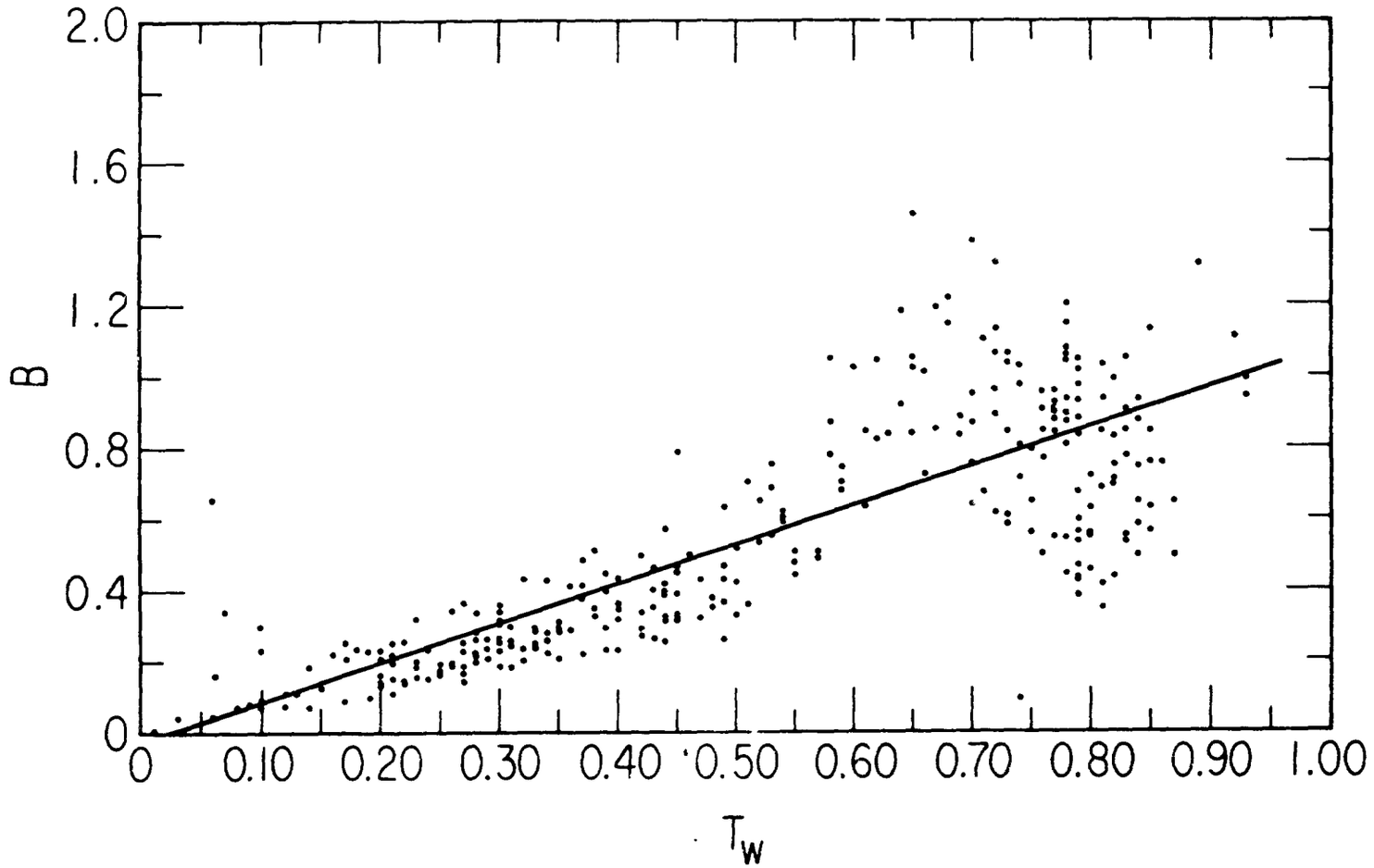

Figure 13. Plot of T_w vs B Showing Linear Least-Squares Fitted Line

Table 8. Least-Squares Fitted Relationships Between T_n, T_w, A, and B

T_n vs A:	A =	$-0.0056 + 0.89 \times T_n$ [correlation coefficient = 0.98]
T_w vs A:	A =	$-0.0026 + 0.0126 \times T_w$ ($T_w < 0.54$) [correlation coefficient = 0.24]
	A =	$-1.0427 + 1.92 \times T_w$ ($T_w \geq 0.54$) [correlation coefficient = 0.76]
T_w vs B:	B =	$-0.0281 + 1.09 \times T_w$ [correlation coefficient = 0.77]
T_w vs T_n:	T_n =	$-0.00417 + 0.029 \times T_w$ ($T_w < 0.54$) [correlation coefficient = 0.45]
	T_n =	$-1.190 + 2.19 \times T_w$ ($T_w \geq 0.54$) [correlation coefficient = 0.84]

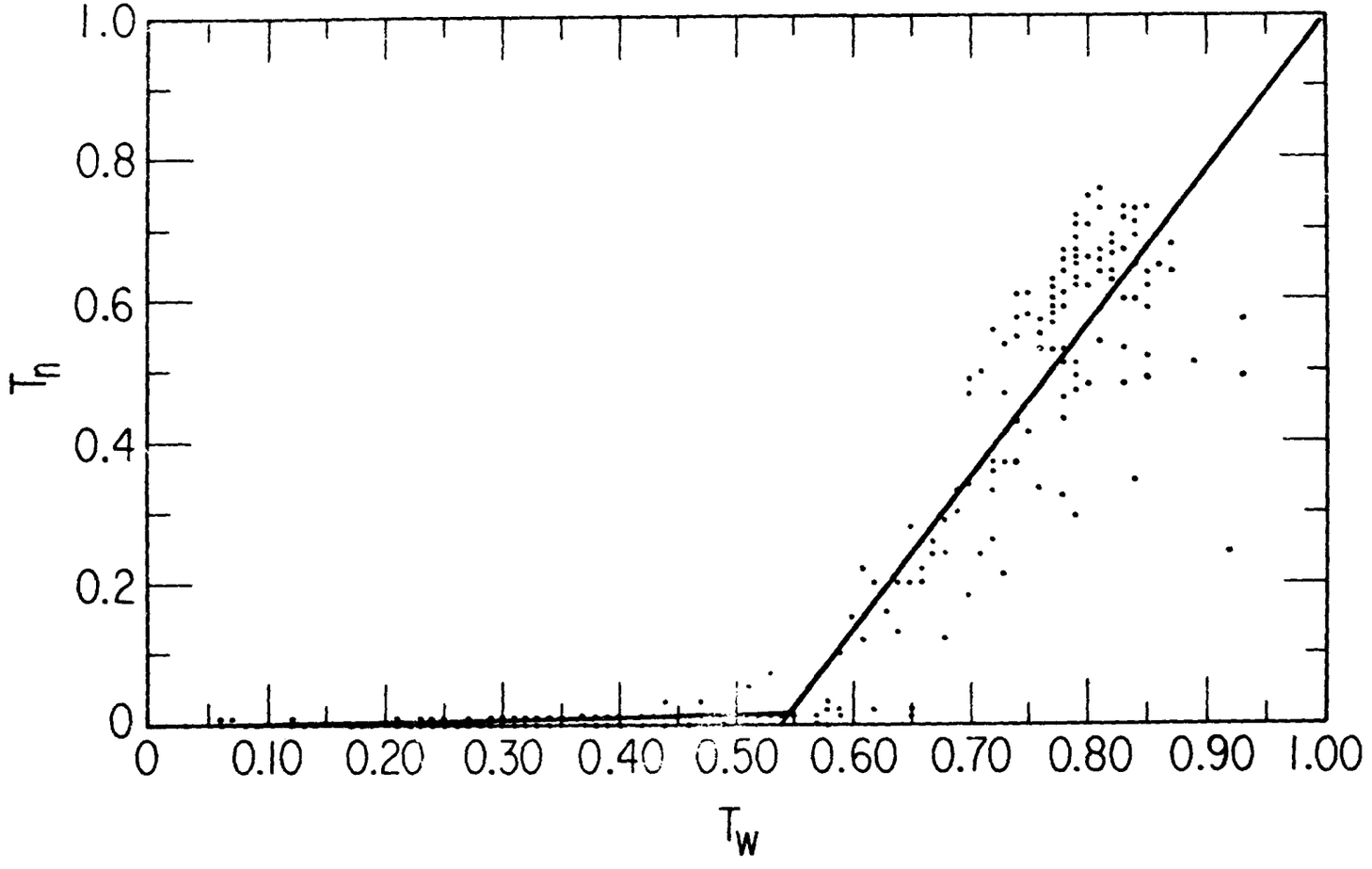

Figure 14. Plot of T_w vs T_n

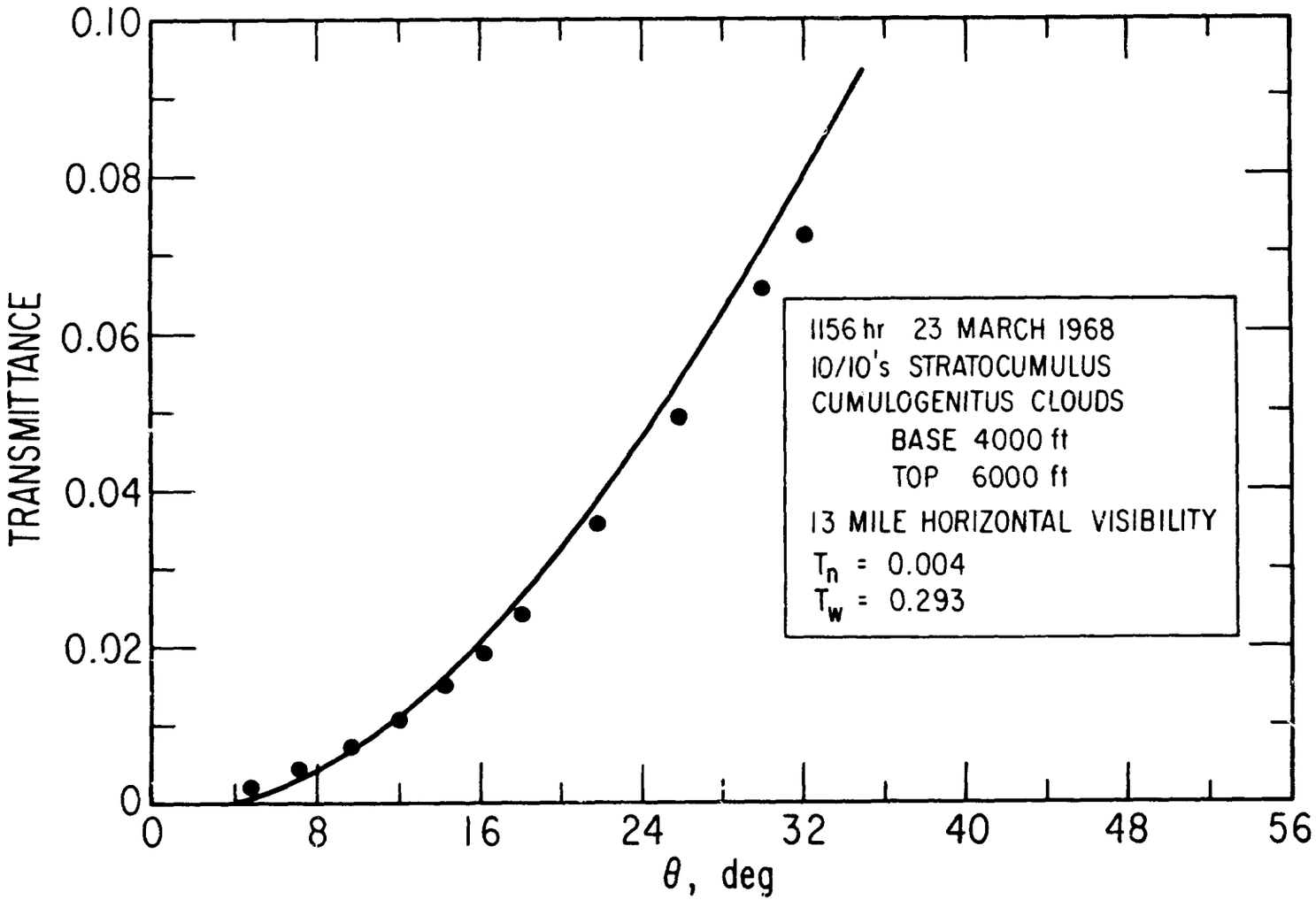

Figure 15a. Sample Plot Showing Accuracy of Model

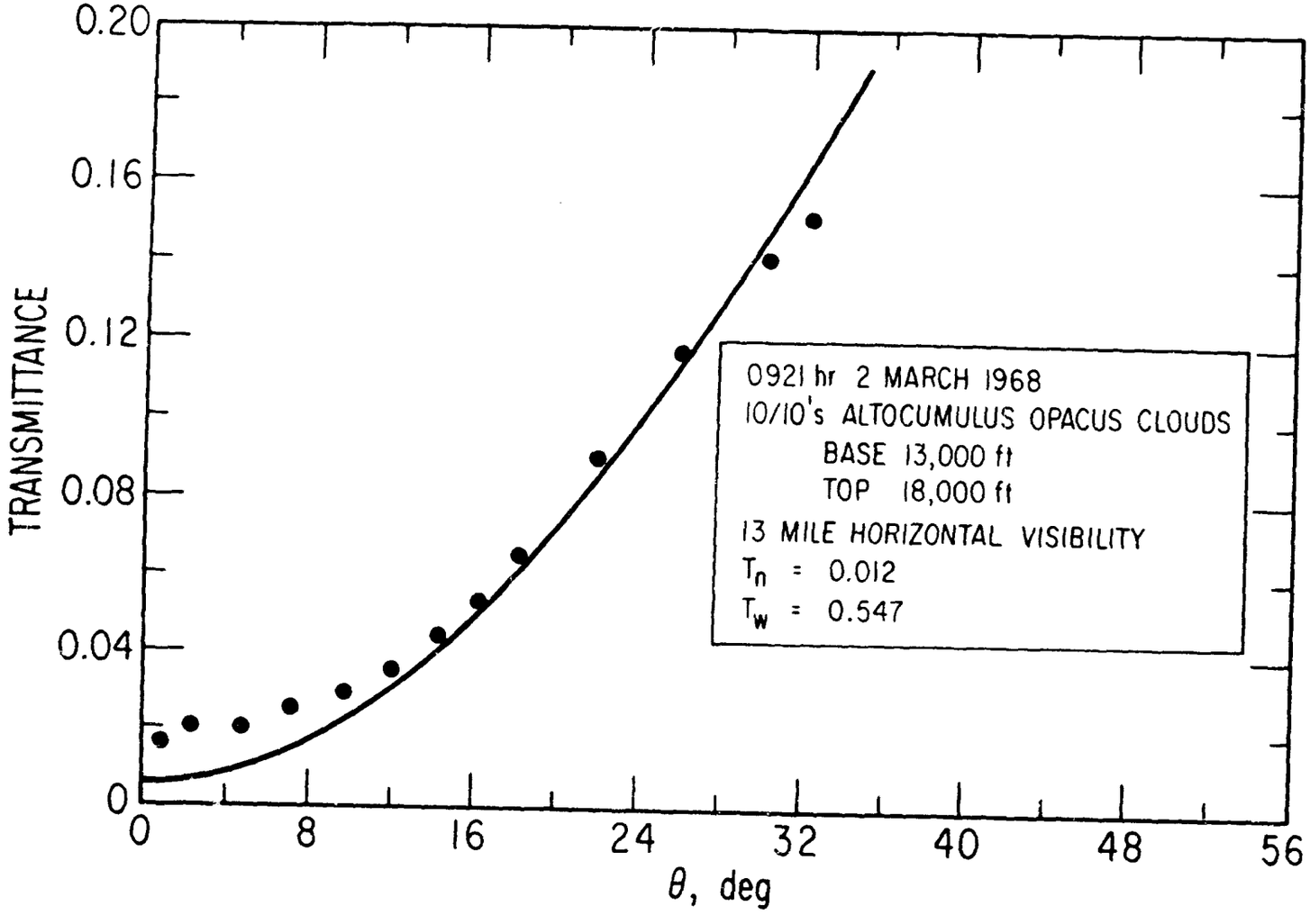

Figure 15b. Sample Plot Showing Accuracy of Model

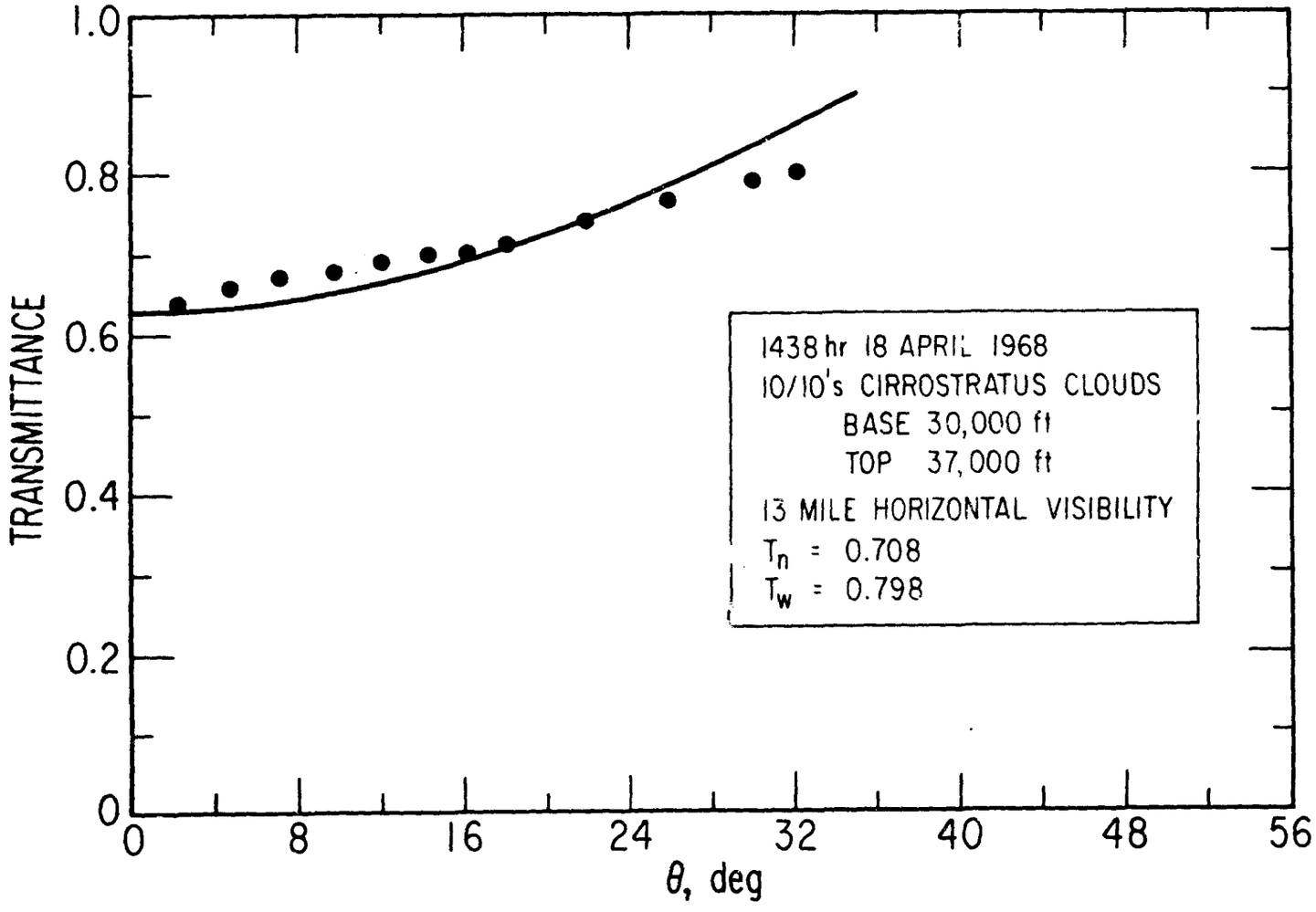

Figure 15c. Sample Plot Showing Accuracy of Model

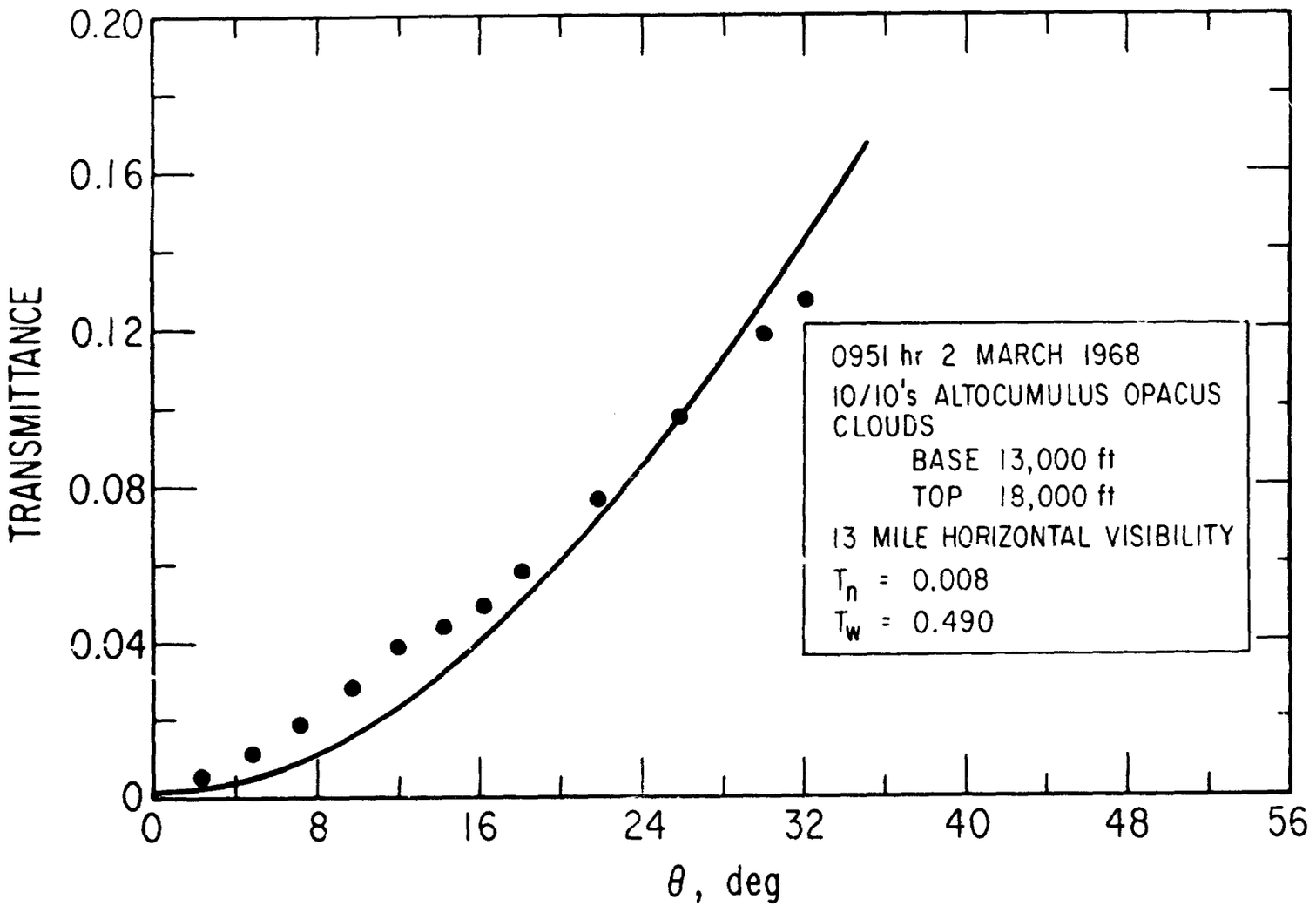

Figure 15d. Sample Plot Showing Accuracy of Model

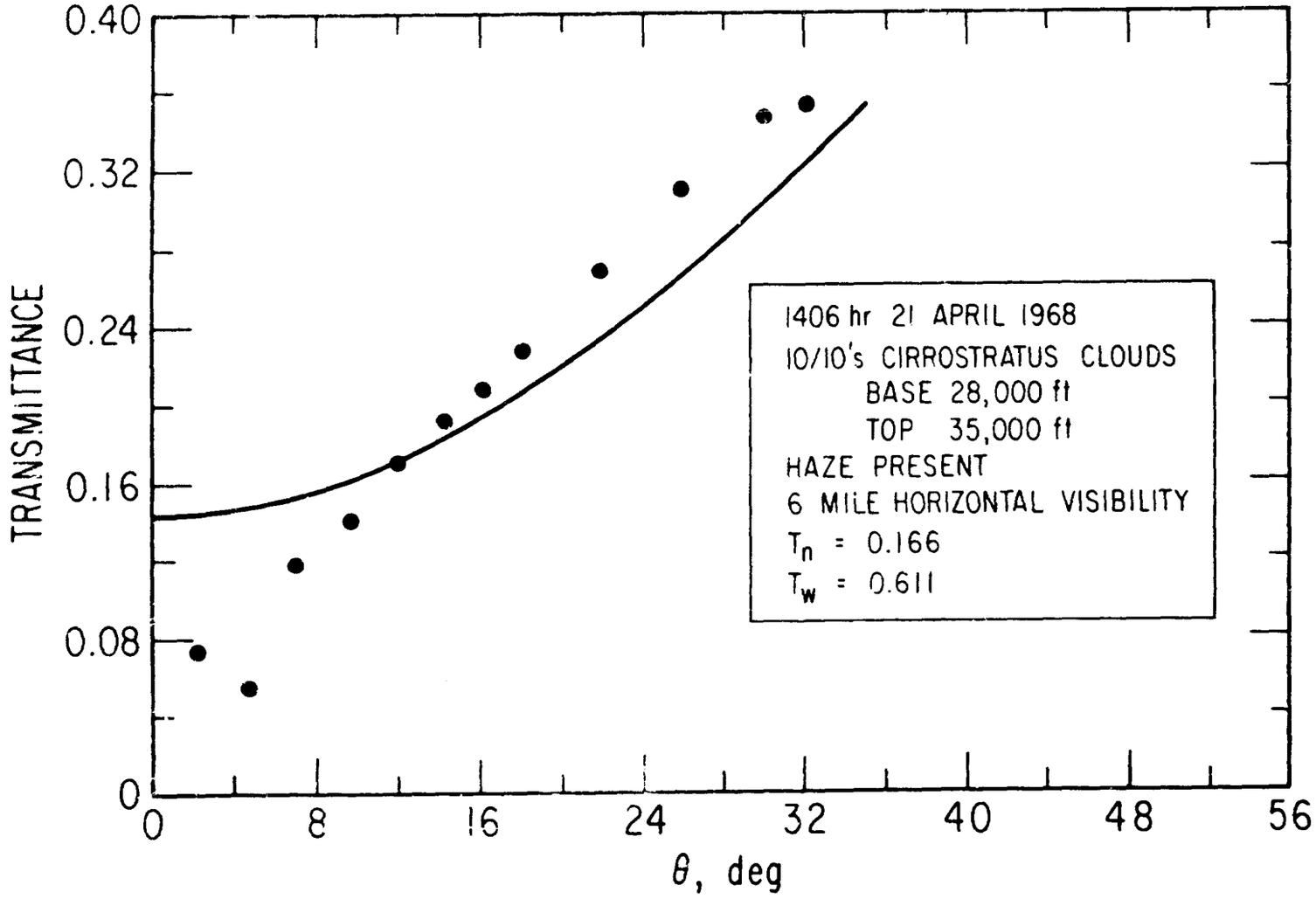

Figure 15e. Sample Plot Showing Accuracy of Model

with the observed points is quite satisfactory. An estimate of the accuracy of a calculated transmittance is ±0.02 or ±10%, whichever is greater.

VII. INTERPRETATION AND APPLICATION

A. INTERPRETATION

The success of the angular scattering model developed here is really a validation of the idea that the transmission of light through the atmosphere has two components: a direct component and a scattered component, and that these two components are separable. The relative magnitudes of the two components varies with the characteristics of the scattering media in the light beam. The direct component is important only when the wide-angle transmittance of the scattering media is greater than roughly 0.50.

Diffuse radiation is usually taken to mean an intensity decrease with the cosine of the angle to the normal of the surface from which the radiation emerges. Such a surface appears equally bright from all directions because this cosine dependence just compensates for the foreshortening of the surface as seen by the observer. The diffuse component of T, B $\sin^2\theta$, which was calculated from this experiment would have been simpler to explain if the measurements could have been made by observing at the zenith so that the vector to the sun would have been perpendicular to the cloud layer. Then θ would have been the ray angle from the cloud normal. However, the minimum solar zenith angle during the experiment was about 12° and measurements were necessary at still larger zenith angles (to 55°) to obtain a reasonable data sample. Because a diffuse surface appears equally bright in all directions, the readings obtained for the diffuse components are still properly made. Note, however, that for nonzero solar zenith angles, the path length of the radiation through the cloud increases and the transmittance decreases. This is borne out qualitatively by the diurnal plots of T_w (denoted PPT) in Ref. 1.

It should be possible to relate T_w and T_n directly to A and B. Indeed $T = T_w$ for $\theta = 90^o$ and $T = T_n$ for $\theta = 2.85^o$. If we use these relations to evaluate A and B we find that:

$$T \simeq T_n + (T_w - T_n) \times \sin^2\theta$$

These values of A and B do not correlate with the experimental data as well as those deduced above. Possible partial explanations for this discrepancy include:

1. The cloud scattering instrument measures in the spectral band from about 0.35 to 0.57 microns with an S-11 photomultiplier response. The pyrheliometers are thermal detectors which respond to all wavelengths transmitted by the atmosphere and by their glass envelopes or windows, i.e. from about 0.35 to 2.5 microns. The scattering properties of the cloud droplets are wavelength dependent.

2. The corrections for atmospheric absorption used in the normalizations are not the same for the two types of instruments.

3. The model was derived only for $\theta \leq 35^o$. An extrapolation of the model to $\theta = 90^o$ is of unknown accuracy.

B. APPLICATION

The model derived for the angular scattering profile of visible solar radiation through clouds has several possible limitations on its validity and applicability. The primary limitation is that the model is valid only for single, overcast cloud layers. Multiple cloud layers cannot be treated for the simple reason that the light impinging on the second layer after emerging from the first layer no longer can be considered to be collimated. Rather it has a scattered component that will diffusely illuminate the second layer, thereby grossly deviating from the conditions of the model.

Likewise the model is inapplicable for broken clouds even with the source behind one of the clouds. The direct component is affected by the presence of broken clouds to the same extent as it was for an overcast layer. However, the scattered component will be grossly changed because of the non-uniform scattering medium. The change can be either to increase or decrease the apparent scattered component. The increase could result from strong reflections off the sides of the clouds into the field of view of the sensor. A decrease might result from a fortuitous arrangement of the clouds so as to preferentially scatter the beam away from the sensor with little or no scattering back into the beam. Such a case might be a single small cloud directly in front of the source with no other clouds in the sky.

A further limitation is that the model is applicable only to collimated light. Diverging or converging light might deviate wildly from the results predicted by the model. This aspect of the model is subject to experimental verification albeit with considerable difficulty.

What has been developed here is a model which describes the angular scattering characteristics of collimated visible light through a single, overcast layer of clouds. The model gives satisfactory agreement with experimental observations. The model should be of great use in the evaluation and prediction of the performance of visible light optical systems in the presence of clouds. It should also serve as a useful stepping off point for the development of models of more complex situations such as broken clouds or multiple cloud layers. It should also serve as a useful test for the theoretical models of collimated light incident on an infinite scattering layer.

REFERENCES

1. R. T. Hall, "Soviet Actinometric Data, Vols. I and II," TR-1001(2129)-1. Vol. I and II, The Aerospace Corp. (April 1967).

2. For example see:
   S. Fritz, J. Meteor. 15, 51 (1958).
   G. K. Il'ich and A. P. Ivanov, Izv., Atmos. and Oceanic Phys. Series, 1, 589 (1965).
   L. M. Romanov, Izv., Atmos. and Oceanic Phys. Series, 1, 599 (1965).
   S. Twomey, H. Jacobowitz, and H. B. Howell, J. Atmos. Sci. 24, 70 (1967).
   G. N. Plass and G. W. Kattawar, App. Optics 7, 361, 415, 699, 869, 1129, 1519 (1968).
   J. E. Hansen, J. Atmos. Sci. 26, 478 (1969).
   R. E. Danielson, D. R. Moore and H. C. van de Hulst, J. Atmos. Sci. 26, 1078 (1969).

3. B. Haurwitz, J. Meteor. 2, 154 (1945); 3, 123 (1946); 5, 110 (1948).

4. M. G. Gibbons, J. Opt. Soc. Am. 49, 702 (1959).

5. M. G. Gibbons, J. R. Nichols, F. I. Laughridge, and R. L. Rudkin, J. Opt. Soc. Am. 51, 633 (1961).

6. M. G. Gibbons, F. I. Laughridge, J. R. Nichols, and N. A. Krause, J. Opt. Soc. Am. 52, 38 (1962).

7. A. Arnulf, J. Bricard, E. Curé, and C. Véret, J. Opt. Soc. Am. 47, 491 (1957).

8. M. Neiburger, J. Meteor. 6, 98 (1949).

9. A Griggs and W. A. Marggraf, "Measurement of Cloud Reflectance Properties and the Atmospheric Attenuation of Solar and Infrared Energy," AFCRL-68-0003, General Dynamics/Convair, San Diego, (December 1967).

10. W. A. Marggraf and M. Griggs, J. Atmos. Sci. 26, 469 (1969).

11. RCA Phototube and Photocells, Technical Manual PT-60, Radio Corporation of America, Electronic Components and Devices, Lancaster, Pennsylvania (1963).

12. Manual of Radiation Observations, United States Weather Bureau, Washington, D.C. (July 1962).

13. "Preliminary Operational Application Techniques for AN/TPQ-11," Air Weather Service Technical Report 180 (September 1964).

14. A. J. Kantor, "Cloud Detection Capability of Operational AN/TPQ-11 Radar Sets During 1966-1967," AFCRL Instrumentation Paper No. 142, AFCRL-68-0269 (May 1968).

15. Manual of Surface Observations (Weather Bureau, Air Force, Navy), Circular N, 7th Edition (Revised), Government Printing Office, Washington, D.C. (April 1966).

16. Solar Radiation, ed. Nathan Robinson, American Elsevier Publishing Co., New York (1966).

APPENDIX

EGLIN DATA FOR 10/10's COVER SORTED BY CLOUD TYPE

A listing of all 334 data samples is shown on the following pages.

EGLIN CLOUD DATA FOR 10/10THS COVER SORTED BY CLOUD TYPE

CLOUD TYPE	DAY	TIME	BASE	TOP	WEATHER	HORZ. VISIB.	T_nx100	T_wx100	NO. OF MISSING APERTURES	SOLAR ELEV. ANGLE	C(1)	C(2)	FIT
L?	118	1254	300	30000	-XTRWF	.6	0	1	2	67.12	0.000	.3046	GOOD
L?	118	1244	300	30000	-XTRW-F	.8	0	1	2	68.62	0.000	.0121	FAIR
L?	118	1234	400	30000	-XF	.8	0	3	2	69.98	0.000	.0430	GOOD
L4	83	1306	4000	7500	RW--	13.0	0	20	2	54.91	0.000	.1579	GOOD
L4	83	1156	4000	6000		13.0	0	29	2	59.38	0.000	.2608	GOOD
L4	83	1256	4000	7500	RW--	13.0	0	38	2	56.13	0.000	.5077	FAIR
L4	83	1206	4000	6000		13.0	1	43	2	60.10	0.000	.4541	FAIR
L4	83	1316	4000	7500	RW--	13.0	2	45	2	53.57	0.000	.7869	FAIR
L5	83	1026	4000	9000		13.0	0	20	2	54.99	0.000	.2079	GOOD
L5	83	1036	4000	9000		13.0	0	21	2	56.12	0.000	.2166	GOOD
L5	83	956	4000	9000		13.0	0	21	2	50.60	0.000	.1922	GOOD
L5	69	949	500	2000	-XF	1.5	0	27	2	35.10	0.000	.1414	GOOD
L5	80	1144	600	3000	F	4.0	0	28	2	59.29	0.000	.2571	FAIR
L5	80	1134	600	3000	F	4.0	0	30	2	59.16	0.000	.3086	GOOD
L5	83	926	4000	8000		13.0	0	33	2	45.58	0.000	.2799	GOOD
L5	57	909	2800	4200		7.0	0	35	2	35.32	0.000	.1986	GOOD
L5	80	1124	600	3000	F	4.0	0	37	3	58.85	0.000	.3682	GOOD
L5	83	1006	4000	9000		13.0	1	40	2	52.13	0.000	.3529	FAIR
L5	83	946	4000	8000		13.0	1	40	2	48.99	0.000	.3134	GOOD
L5	83	1046	4000	7000		13.0	1	42	2	57.22	0.000	.4927	GOOD
L5	83	936	4000	8000		13.0	0	42	2	47.32	0.000	.2649	GOOD
L5	89	831	1500	2000		9.0	1	44	2	36.62	0.000	.2474	GOOD
L5	89	901	1500	2000		9.0	1	45	2	42.54	0.000	.3799	FAIR
L5	83	1056	4000	6000	S--	13.0	1	46	2	58.18	0.000	.4937	GOOD
L5	89	851	1500	2000		9.0	1	46	2	40.60	0.000	.4031	GOOD
L5	89	841	1500	2000		9.0	1	48	2	38.62	0.000	.3701	GOOD
L5	134	947	1600	2500		13.0	1	50	2	58.36	0.000	.4170	FAIR
L5	89	911	1500	2000		9.0	1	52	2	44.45	0.000	.5288	FAIR
L5	83	916	4000	8000		13.0	1	54	2	43.79	0.000	.5960	GOOD
L5	83	836	4000	10000		13.0	1	54	2	36.19	.008	.5967	FAIR
L5	134	907	1400	2500		13.0	1	55	1	52.05	0.000	.4372	FAIR
L5	83	1116	4000	6000	S--	13.0	4	55	1	59.63	.242	.9369	POOR
L5	134	857	1400	2500		13.0	1	57	2	49.91	0.000	.4800	GOOD
L5	134	917	1600	2500		13.0	0	57	1	54.17	.006	.4991	GOOD
L5	89	921	1500	2000		9.0	3	58	2	46.31	.016	.7797	FAIR

L5	80	1054	600	2000		7.0	0	58	0	56.90	0.000	.8699	GOOD
L5	134	927	1600	2500		13.0	2	60	1	56.27	.047	.7504	POOR
L5	83	856	4000	8000		13.0	1	60	2	40.07	.015	.5318	POOR
L5	134	947	1600	2500		13.0	2	62	1	60.43	.024	.8208	GOOD
L5	83	1106	4000	6000	S--	13.0	5	70	2	58.99	.035	1.3886	FAIR
L5	83	906	4000	8000		13.0	15	77	2	41.95	0.000	2.0548	POOR
L5	57	919	2800	4200		7.0	51	89	0	36.94	.343	1.3204	FAIR
L6	70	853	400	2300	F	2.0	0	6	2	36.09	0.000	.1645	GOOD
L6	46	1231	1700	15000	RW-F	2.0	0	6	2	45.13	0.000	.0495	GOOD
L6	46	1301	1700	21000	R-F	1.2	0	6	2	42.86	0.000	.0458	GOOD
L6	70	953	000	2500		7.0	1	6	2	46.07	0.000	.6624	GOOD
L6	70	923	1000	2000	F	4.0	1	7	2	41.35	.003	.3464	FAIR
L6	46	1221	2000	14000	RW-	4.0	0	8	1	45.64	0.000	.0739	GOOD
L6	46	1241	1700	15000	RW-F	1.5	0	9	2	44.49	0.000	.0742	GOOD
L6	46	1051	2200	50000	RW--	10.0	0	9	1	44.48	0.000	.0927	GOOD
L6	46	1031	2300	14000	RW--	10.0	0	9	1	42.86	0.000	.0770	GOOD
L6	46	1251	1700	23000	R-F	1.5	0	10	1	43.73	0.000	.0737	GOOD
L6	46	1121	2200	20000	RW-	7.0	0	10	1	46.03	0.000	.0920	GOOD
L6	70	913	600	2000	F	4.0	1	10	1	39.65	.002	.2980	GOOD
L6	46	1211	2000	14000	RW-	4.0	0	10	1	46.04	0.000	.0886	GOOD
L6	70	903	400	2000	F	3.0	1	10	2	37.89	0.000	.2376	FAIR
L6	46	1151	2000	22000	RW-	4.0	0	12	1	46.43	0.000	.1103	GOOD
L6	46	1111	2200	13000	RW-	7.0	1	12	1	45.64	0.000	.1066	GOOD
L6	46	1001	2500	13000		13.0	0	12	1	39.65	0.000	.0752	GOOD
L6	46	1131	2200	19000	RW-	7.0	0	12	1	46.30	0.000	.1156	GOOD
L6	46	1231	2000	14000	RW-	4.0	0	13	1	46.30	0.000	.1030	GOOD
L6	118	894	400	2500	-XF	.2	0	14	2	36.50	0.000	.0727	GOOD
L6	71	1317	300	2500	XF	.9	0	14	2	49.44	.001	.1849	GOOD
L6	46	1141	2200	20000	RW-	7.0	0	15	1	46.43	0.000	.1239	GOOD
L6	71	1307	300	2500	XF	.9	0	16	2	50.66	0.000	.2185	GOOD
L6	71	1237	300	2500	XF	.9	0	17	2	53.65	0.000	.2533	FAIR
L6	118	904	500	1500	-XF	1.5	0	17	2	49.22	0.000	.0867	GOOD
L6	71	1257	300	2500	XF	.9	0	17	2	51.78	0.000	.2050	GOOD
L6	71	1247	300	2500	XF	.9	0	18	2	52.78	0.000	.2345	GOOD
L6	71	1327	300	2500	XF	.9	0	19	2	48.11	.001	.2295	GOOD
L6	118	814	400	2500	-XF	.2	0	19	2	38.64	0.000	.0997	GOOD
L6	47	926	800	2500	H	5.0	0	19	2	35.22	0.000	.0950	GOOD
L6	71	1337	300	2000	XF	.9	0	20	2	46.69	0.000	.2295	GOOD
L6	70	933	000	2000	F	4.0	1	20	2	42.99	.009	.4046	POOR
L6	46	1011	2300	14000	RW-	10.0	0	20	1	40.81	0.000	.1355	GOOD
L6	99	850	400	2000	-XF	2.5	0	20	2	42.70	0.000	.1294	GOOD
L6	47	936	800	2500	H	5.0	0	21	2	36.66	0.000	.1097	GOOD

L6	47	1016	900	2500	H	6.0	1	21	2	41.67	0.000	.1491	GOOD
L6	71	1347	300	2000	XF	.9	0	21	2	45.20	0.000	.2498	GOOD
L6	47	956	800	2500	H	6.0	0	22	2	39.33	0.000	.1321	GOOD
L6	71	1357	300	1500	XF	.9	0	22	2	43.62	0.000	.2532	GOOD
L6	47	1006	800	2500	H	6.0	0	22	2	40.54	0.000	.1380	GOOD
L6	71	1327	300	2000	XF	.9	0	23	2	54.38	0.000	.3196	GOOD
L6	47	946	800	2500	H	5.0	0	23	1	38.04	.002	.1275	POOR
L6	47	1026	900	2500	H	6.0	0	23	3	42.70	0.000	.1537	GOOD
L6	47	1036	900	2500	H	6.0	1	23	3	43.62	0.000	.1802	GOOD
L6	69	1049	200	5000	XF	.5	0	24	2	52.40	0.000	.2295	GOOD
L6	118	854	500	1500	-XF	1.8	1	24	2	47.13	0.000	.1466	GOOD
L6	69	929	500	6000	-XF	1.5	0	25	2	42.04	0.000	.1694	FAIR
L6	69	1359	900	5000	-XFH	5.0	0	25	2	42.70	0.000	.1889	GOOD
L6	118	834	400	2500	-XF	.2	1	25	2	42.91	0.000	.1541	GOOD
L6	69	1429	800	5000	-XF	5.0	0	25	2	37.63	0.000	.1590	GOOD
L6	71	1217	300	2000	XF	.9	0	26	2	54.96	0.000	.3406	GOOD
L6	69	949	500	6000	-XF	1.5	0	26	2	45.17	0.000	.1879	GOOD
L6	69	1019	400	6000	-XF	.6	0	26	2	49.25	0.000	.1832	GOOD
L6	71	1207	300	2000	XF	.9	0	27	2	55.38	0.000	.3588	GOOD
L6	47	1046	1000	2500	H	6.0	1	27	3	44.44	0.000	.2031	GOOD
L6	47	1116	1000	2500	H	6.0	1	27	3	46.19	0.000	.2231	GOOD
L6	69	1419	900	5000	-XFH	5.0	0	27	2	39.38	0.000	.1630	GOOD
L6	71	1407	300	1500	XF	.9	0	27	2	41.99	0.000	.2504	FAIR
L6	69	1409	800	5000	-XFH	5.0	0	27	2	41.97	0.000	.1829	GOOD
L6	71	1427	200	1500	XF	.4	0	28	2	38.54	.001	.1350	GOOD
L6	71	1437	200	1500	XF	.4	0	28	1	36.74	0.000	.2086	FAIR
L6	69	1109	300	7000	XF	1.0	0	28	2	53.86	0.000	.2767	FAIR
L6	47	1146	1000	2500	H	6.0	1	29	2	46.79	0.000	.2299	GOOD
L6	69	939	500	6000	-XF	1.5	0	29	2	43.64	0.000	.2019	GOOD
L6	47	1056	1000	2500	H	6.0	0	30	2	45.14	0.000	.2225	GOOD
L6	118	824	400	2500	-XF	.2	1	30	2	40.78	0.000	.1779	GOOD
L6	96	1248	1000	2700		7.0	0	30	2	61.53	0.000	.3340	FAIR
L6	47	1136	1000	2500	H	6.0	0	30	3	46.72	0.000	.2466	GOOD
L6	69	1319	900	5000	-XFH	5.0	0	30	2	48.51	0.000	.2597	GOOD
L6	69	1259	800	5000	-XFH	5.0	0	31	2	50.86	0.000	.2920	FAIR
L6	69	919	500	2500	-XF	1.5	0	31	1	40.39	.001	.1797	FAIR
L6	47	1126	1000	2500	H	6.0	0	31	3	46.52	0.000	.2376	GOOD
L6	47	1156	1000	2500	H	6.0	1	31	2	46.72	0.000	.2538	GOOD
L6	118	844	500	2500	-XF	.6	1	32	2	45.03	0.000	.1950	GOOD
L6	71	1157	300	1000	XF	.9	0	32	2	55.65	0.000	.4234	GOOD
L6	47	1256	1200	2500	H	6.0	0	32	2	43.63	0.000	.2297	GOOD
L6	47	1216	1000	2500	H	6.0	0	33	2	46.19	0.000	.2445	GOOD

L6	71	1417	300	1500	XF	.5	0	33	3	40.29	.003	.2310	FAIR
L6	47	1206	1000	2500	H	6.0	1	33	3	46.52	0.000	.2876	FAIR
L6	71	1147	300	1000	XF	.9	0	34	2	55.75	0.000	.4245	FAIR
L6	47	1226	1000	2500	H	6.0	1	34	2	45.73	0.000	.2757	GOOD
L6	99	930	600	2000	F	4.0	0	34	2	50.53	0.000	.2519	GOOD
L6	47	1106	1000	2500	H	6.0	1	35	2	45.73	0.000	.2957	FAIR
L6	47	1236	1000	2500	H	6.0	1	35	2	45.15	0.000	.2790	GOOD
L6	69	1009	400	6000	-XF	.6	0	35	2	47.98	0.000	.2797	GOOD
L6	69	1009	400	6000	-XF	.6	0	35	2	50.41	0.000	.3045	GOOD
L6	96	1158	1000	2700		7.0	0	36	2	65.37	0.000	.4062	FAIR
L6	47	1246	1000	2500	H	6.0	0	36	2	44.45	0.000	.2812	GOOD
L6	71	1137	200	1000	XF	.9	1	37	2	55.68	0.000	.4801	GOOD
L6	99	940	700	2000	F	6.0	1	38	2	52.39	0.000	.3203	GOOD
L6	69	1059	200	5000	XF	.6	0	38	2	53.20	0.000	.3458	FAIR
L6	69	1219	600	7000	-XFH	3.0	0	39	2	54.08	0.000	.4425	GOOD
L6	47	1406	1200	2000	H	6.0	1	39	2	35.23	.001	.2243	GOOD
L6	69	1248	800	5000	-XFH	5.0	0	39	2	51.86	0.000	.3918	GOOD
L6	69	909	500	2500	-XF	1.5	0	40	1	38.67	0.000	.2259	GOOD
L6	96	1238	1000	2700		7.0	0	40	1	62.66	0.000	.4309	GOOD
L6	47	1316	1200	2500	H	6.0	0	42	2	41.67	0.000	.3336	GOOD
L6	47	1706	1200	2500	H	6.0	0	42	2	42.70	0.000	.2949	FAIR
L6	96	1218	1000	2700		7.0	1	42	1	64.41	0.000	1.0040	FAIR
L6	99	950	700	2000		7.0	1	43	2	54.19	0.000	.3324	GOOD
L6	47	1756	1200	2000	H	6.0	1	43	2	36.67	0.000	.2546	FAIR
L6	69	1329	800	5000	-XFH	5.0	1	44	2	47.18	0.000	.3981	GOOD
L6	69	959	400	6000	-XF	1.5	0	44	2	46.61	0.000	.3176	FAIR
L6	69	1439	600	5000	-XF	5.0	0	44	2	35.84	0.000	.3075	FAIR
L6	69	1119	400	8000	XF	1.5	1	44	2	54.37	0.000	.4117	FAIR
L6	69	1149	400	6000	-XF	2.2	1	44	2	54.95	.006	.5659	GOOD
L6	47	1326	1200	2500	H	6.0	1	45	2	40.55	.001	.3255	GOOD
L6	69	1709	800	5000	-XFH	5.0	1	45	2	49.74	0.000	.4591	GOOD
L6	47	1336	1200	2500	H	6.0	1	45	3	39.34	0.000	.3051	GOOD
L6	99	1000	700	2000		7.0	1	45	2	55.93	0.000	.4448	GOOD
L6	48	930	1200	1800		7.0	1	47	2	36.08	0.000	.3125	FAIR
L6	96	1208	1000	2700		7.0	1	49	0	64.99	.002	.6302	GOOD
L6	69	1349	800	5000	-XFH	5.0	0	49	2	44.27	0.000	.4633	GOOD
L6	111	806	1600	2500	H	6.0	1	49	1	35.81	.001	.2555	GOOD
L6	47	1346	1200	2500	H	6.0	0	50	2	38.05	0.000	.3197	FAIR
L6	69	1229	600	5000	-XFH	3.0	1	52	1	53.48	0.000	.6492	FAIR
L6	69	1339	800	5000	-XFH	5.0	1	53	2	45.76	0.000	.5483	GOOD
L6	69	1239	600	5000	-XFH	3.0	1	53	2	52.74	0.000	.7501	FAIR
L6	69	1129	400	8000	XF	1.5	1	54	1	54.72	.002	.6163	GOOD

L6	48	940	1200	1800		7.0	1	55	3	37.51	.005	.4704	FAIR
L6	48	950	1200	1800		7.0	1	59	2	38.96	0.000	.7011	FAIR
L6	69	1139	400	6000	-XF	2.2	2	59	2	54.92	0.000	.7428	GOOD
L6	69	1159	700	6000	-XFH	2.5	1	59	1	54.82	.035	.9372	POOR
L6	48	1000	1400	1800		10.0	1	65	2	40.12	0.000	.8364	GOOD
L6	96	1138	1000	2500		7.0	2	65	2	65.46	0.000	1.4649	FAIR
L6	111	816	1600	2500	H	6.0	25	68	2	37.94	.181	.2343	POOR
L6	111	826	1600	2500	H	6.0	24	92	1	40.06	.097	1.1126	FAIR
M1	59	907	14000	25000		7.0	12	61	1	35.54	.152	.6297	FAIR
M1	59	937	14000	25000		7.0	24	68	1	40.31	.096	1.2239	FAIR
M1	59	917	14000	25000		7.0	48	83	1	37.19	.449	.9056	FAIR
M1	59	947	14000	25000		7.0	65	86	1	41.76	.648	.7555	FAIR
M1	59	927	14000	25000		7.0	57	93	1	38.78	.538	.9425	FAIR
M3	90	1055	15000	20000	GF	5.0	2	58	0	60.64	.005	1.0549	GOOD
M3	90	1145	15000	20000	GF	5.0	12	68	1	63.22	.203	1.1434	FAIR
M3	90	1105	15000	20000	GF	5.0	10	73	1	61.53	.167	1.0648	FAIR
M3	90	1115	15000	20000	GF	5.0	11	76	1	62.24	.161	1.0646	POOR
M3	90	1125	15000	20000	GF	5.0	49	85	1	62.77	.134	2.7925	FAIR
M7	62	1041	13000	18000		13.0	0	23	1	49.16	0.000	.1946	GOOD
M7	62	1031	13000	18000		13.0	0	28	1	48.19	0.000	.2155	FAIR
M7	62	1131	8000	20000		13.0	0	28	2	52.08	0.000	.3321	GOOD
M7	62	1141	8000	20000		13.0	1	30	2	52.24	0.000	.3542	FAIR
M7	62	1121	8000	20000		13.0	0	30	2	51.78	0.000	.2998	GOOD
M7	62	1051	8000	20000		13.0	0	34	1	50.02	0.000	.3476	GOOD
M7	62	901	13000	18000		13.0	0	37	1	35.35	0.000	.2113	GOOD
M7	62	1021	13000	18000		13.0	0	37	1	47.10	0.000	.4088	GOOD
M7	62	1111	8000	20000		13.0	0	42	2	51.33	0.000	.3279	GOOD
M7	62	1101	8000	20000		13.0	1	43	1	50.74	0.000	.3447	GOOD
M7	62	931	13000	18000		13.0	1	45	1	40.29	0.000	.3164	GOOD
M7	62	1001	13000	18000		13.0	1	48	1	44.63	.003	.3442	GOOD
M7	62	941	13000	18000		13.0	1	49	3	41.81	0.000	.3590	GOOD
M7	62	951	13000	18000		13.0	1	49	1	43.26	.014	.4239	FAIR
M7	62	1011	13000	18000		13.0	1	50	1	45.92	.001	.5079	GOOD
M7	62	911	13000	18000		13.0	1	51	3	37.05	.002	.3514	GOOD
M7	62	921	13000	18000		13.0	1	55	0	38.70	.016	.4996	GOOD
H1	42	1213	UNKN.	THIN		10.0	29	66	1	44.65	.334	.4328	POOR
H1	42	1243	UNKN.	THIN		10.0	32	70	0	43.07	.468	.6386	POOR
H1	42	1223	UNKN.	THIN		10.0	51	78	1	44.25	.408	1.1533	FAIR
H1	42	1203	UNKN.	THIN		10.0	69	84	0	44.93	.681	.5786	FAIR
H1	42	1153	UNKN.	THIN		10.0	71	84	0	45.09	.711	.6440	FAIR
H7	112	1526	25000	35000	H	6.0	0	27	2	36.00	0.000	.1363	GOOD
H7	112	1516	25000	35000	H	6.0	0	31	1	38.13	0.000	.1768	GOOD

H7	112	1506	25000	35000	H	6.0	0	34	1	40.25	0.000	.2160	GOOD
H7	112	1456	25000	35000	H	6.0	1	39	1	42.36	.003	.2961	GOOD
H7	112	1436	24000	35000	H	6.0	1	40	2	46.54	.002	.3415	GOOD
H7	112	1446	24000	35000	H	6.0	3	44	2	44.46	.015	.3762	GOOD
H7	112	1426	25000	35000	H	6.0	3	47	3	48.60	.054	.4230	GOOD
H7	110	1258	29000	36000	H	6.0	5	51	1	64.43	.035	.6986	GOOD
H7	110	1308	29000	36000	H	6.0	7	53	1	62.87	.059	.6843	GOOD
H7	119	1212	18000	22000		13.0	7	56	1	72.56	.072	.7804	POOR
H7	42	1333	22000	28000		10.0	10	59	1	38.27	.112	.6768	FAIR
H7	119	1242	18000	22000		13.0	15	60	2	69.17	.092	1.0261	FAIR
H7	51	1403	25000	30000		13.0	11	61	1	36.79	.104	.8333	POOR
H7	112	1406	26000	35000	H	6.0	17	61	1	52.64	.105	1.0029	POOR
H7	112	1356	31000	33000	H	6.0	22	61	2	54.62	.222	.8445	FAIR
H7	110	1248	26000	31000	H	6.0	20	62	1	65.88	.210	1.0492	FAIR
H7	110	1318	29000	36000	H	6.0	16	63	2	61.20	.143	.8373	FAIR
H7	119	1232	18000	22000		13.0	17	63	1	70.50	.138	1.1531	POOR
H7	119	1202	18000	22000		13.0	13	64	1	73.21	.081	1.1988	FAIR
H7	110	1328	29000	36000	H	6.0	20	64	3	59.44	.137	.9212	FAIR
H7	119	1252	17000	20000		13.0	20	65	2	67.67	.149	1.0564	GOOD
H7	110	1108	29000	31000	H	6.0	28	65	1	68.72	.233	1.0254	GOOD
H7	129	1443	29000	33000		11.0	21	65	1	47.64	.191	.7530	POOR
H7	119	1152	18000	22000		13.0	22	66	1	73.56	.168	1.0104	FAIR
H7	112	1416	27000	35000	H	6.0	20	66	2	50.63	.211	.7199	GOOD
H7	119	1312	17000	20000		10.0	24	67	1	64.33	.140	1.1976	FAIR
H7	129	1413	29000	33000		11.0	26	67	2	53.99	.190	.8491	GOOD
H7	110	1238	28000	31000	H	6.0	29	68	1	67.19	.249	1.1517	GOOD
H7	129	1403	29000	33000		11.0	30	69	1	55.08	.197	.8853	GOOD
H7	110	1128	29000	31000	H	6.0	30	69	3	70.19	.315	.8336	GOOD
H7	129	1423	29000	33000		11.0	33	69	1	51.89	.203	.8320	FAIR
H7	42	1343	19000	26000		10.0	18	70	1	37.03	.176	.7500	FAIR
H7	109	1348	30000	33000		10.0	49	70	1	55.52	.490	.6348	FAIR
H7	129	1353	29000	33000		11.0	34	70	2	58.15	.243	.8708	GOOD
H7	41	1007	17000	28000		10.0	29	70	0	38.90	.419	.4201	POOR
H7	129	1103	26000	34000		11.0	47	70	1	73.37	.326	.9538	GOOD
H7	109	1238	30000	35000		10.0	50	71	2	66.89	.529	.6703	FAIR
H7	119	1322	17000	20000		10.0	24	71	1	62.52	.234	1.1065	FAIR
H7	110	1208	28000	31000	H	6.0	35	72	1	69.98	.297	1.0669	FAIR
H7	119	1222	18000	22000		13.0	33	72	1	71.65	.178	1.3242	GOOD
H7	124	819	UNKN.	THIN	H	5.0	26	72	2	40.57	.209	.8884	FAIR
H7	109	1148	32000	35000		10.0	56	72	2	70.28	.572	.6084	FAIR
H7	110	1228	28000	31000	H	6.0	39	72	2	68.33	.296	1.1765	GOOD
H7	112	1346	25000	THIN	H	6.0	37	72	2	56.55	.382	.9617	GOOD

H7	41	937	18000	34000		8.0	21	73	1	35.17	.172	.8438	FAIR
H7	112	1336	25000	THIN	H	6.0	47	73	2	58.44	.532	.6920	GOOD
H7	110	1138	29000	31000	H	6.0	37	73	1	70.55	.340	1.0397	GOOD
H7	109	1138	32000	35000		10.0	54	73	1	70.20	.562	.5776	FAIR
H7	109	1128	32000	38000		10.0	55	74	1	69.85	.518	.8020	FAIR
H7	109	1158	30000	35000		10.0	61	74	1	70.09	.733	.0833	FAIR
H7	110	1048	31000	33000	H	6.0	37	74	2	66.42	.290	1.0327	FAIR
H7	110	1058	29000	31000	H	6.0	43	74	1	67.66	.398	.9796	FAIR
H7	109	1728	30000	35000		10.0	58	74	2	68.01	.590	.7111	FAIR
H7	109	1258	30000	33000		10.0	61	75	1	64.16	.598	.6462	FAIR
H7	110	1028	31000	33000	H	6.0	41	75	2	63.59	.396	.7920	FAIR
H7	109	1118	32000	38000		10.0	58	75	3	69.24	.597	.5567	FAIR
H7	109	1338	30000	33000		10.0	57	76	1	57.39	.584	.4924	FAIR
H7	129	1053	26000	34000		11.0	57	76	1	71.93	.410	.9569	GOOD
H7	110	1528	30000	THIN	H	6.0	55	76	2	35.23	.372	.8451	GOOD
H7	124	829	UNKN.	THIN	H	5.0	33	76	2	42.71	.280	.9057	GOOD
H7	42	1033	18000	22000		10.0	53	76	0	41.80	.499	.7662	FAIR
H7	51	1353	26000	32000		13.0	32	76	2	38.24	.385	.8358	POOR
H7	112	1326	25000	THIN	H	6.0	53	77	2	60.27	.531	.8457	FAIR
H7	110	1518	30000	THIN	H	6.0	57	77	3	37.36	.374	.9602	FAIR
H7	110	1458	30000	THIN	H	6.0	59	77	1	41.59	.420	.9805	GOOD
H7	110	1448	30000	34000	H	6.0	59	77	1	43.68	.427	.9101	GOOD
H7	110	1508	30000	THIN	H	6.0	58	77	2	39.48	.415	.9804	GOOD
H7	109	1108	32000	38000		10.0	63	77	2	68.40	.630	.5403	FAIR
H7	110	1418	30000	34000	H	6.0	60	77	2	49.84	.447	.9278	GOOD
H7	125	1033	24000	36000		11.0	62	77	1	68.62	.452	.8799	GOOD
H7	109	1428	30000	37000		13.0	66	77	3	47.62	.609	.5351	POOR
H7	112	1256	25000	THIN	H	6.0	61	78	3	65.23	.693	.4386	GOOD
H7	110	1428	30000	34000	H	6.0	61	78	1	47.81	.446	.9366	GOOD
H7	110	1438	30000	34000	H	6.0	67	78	2	45.75	.458	.8947	GOOD
H7	110	1358	30000	34000	H	6.0	59	78	2	53.81	.493	.8060	GOOD
H7	41	947	18000	34000		8.0	32	78	1	36.49	.254	1.0936	FAIR
H7	112	1306	25000	THIN	H	6.0	64	78	3	63.70	.682	.5393	GOOD
H7	110	1338	29000	36000	H	6.0	46	78	3	57.62	.338	1.0447	GOOD
H7	129	1143	26000	34000		11.0	66	78	1	76.55	.486	.8703	GOOD
H7	110	1038	31000	33000	H	6.0	43	78	1	65.02	.371	1.0631	FAIR
H7	110	1148	29000	31000	H	6.0	53	78	1	70.63	.399	1.2090	FAIR
H7	110	1018	31000	33000	H	6.0	51	79	2	61.86	.424	1.0179	FAIR
H7	109	1358	30000	37000		13.0	69	79	1	53.60	.656	.5561	FAIR
H7	109	1418	30000	37000		13.0	71	79	2	49.64	.697	.4203	GOOD
H7	109	1458	30000	THIN		13.0	63	79	2	41.41	.570	.6704	FAIR
H7	109	1058	32000	38000		10.0	72	79	2	67.35	.710	.4247	GOOD

H7	42	1017	18000	23000		10.0	49	79	0	39.85	.526	.5313	FAIR
H7	109	1528	30000	THIN		13.0	47	79	1	35.06	.392	.8756	FAIR
H7	129	1133	26000	34000		11.0	55	79	1	76.24	.475	.0318	GOOD
H7	109	1448	30000	37000		13.0	67	79	3	43.49	.638	.4260	FAIR
H7	124	1019	UNKN.	THIN		8.0	66	79	2	65.16	.569	.5924	GOOD
H7	129	1027	24000	36000		11.0	63	79	1	66.80	.468	.8829	GOOD
H7	109	1328	30000	33000		10.0	72	79	2	59.20	.726	.3776	GOOD
H7	110	1408	30000	34000	H	6.0	62	79	2	51.84	.456	.9798	GOOD
H7	109	1308	30000	33000		10.0	71	79	1	62.60	.714	.4628	FAIR
H7	42	1353	18000	23000		10.0	29	79	1	35.71	.180	1.0504	FAIR
H7	109	1438	30000	37000		13.0	71	80	1	45.57	.659	.5426	GOOD
H7	124	1009	UNKN.	THIN		8.0	66	80	2	63.29	.583	.6223	GOOD
H7	109	1508	30000	THIN		13.0	62	80	1	39.30	.567	.7141	FAIR
H7	42	953	18000	20000		10.0	48	80	0	37.52	.448	.5514	FAIR
H7	109	1408	30000	37000		13.0	75	80	2	51.64	.711	.4514	GOOD
H7	110	1008	31000	33000	H	6.0	54	81	1	60.14	.456	.9374	GOOD
H7	129	1043	24000	36000		11.0	67	81	2	70.33	.513	.8419	GOOD
H7	124	959	UNKN.	THIN		8.0	64	81	2	61.37	.588	.6835	GOOD
H7	129	1123	26000	34000		11.0	66	81	1	75.58	.465	1.0356	GOOD
H7	124	1049	UNKN.	THIN		8.0	73	81	2	70.22	.732	.3442	GOOD
H7	109	1318	30000	33000		10.0	76	81	2	60.95	.751	.4083	GOOD
H7	124	1039	UNKN.	THIN		8.0	69	82	2	68.64	.659	.4317	GOOD
H7	129	953	24000	36000		11.0	64	82	1	60.98	.463	.9955	FAIR
H7	129	1013	24000	36000		11.0	67	82	1	64.91	.512	.8284	GOOD
H7	42	1043	16000	22000		10.0	68	82	0	42.63	.508	.6907	FAIR
H7	124	949	UNKN.	THIN	H	5.0	67	82	2	59.40	.583	.7482	FAIR
H7	124	939	UNKN.	THIN	H	5.0	63	82	2	57.39	.576	.7055	GOOD
H7	129	1003	24000	36000		11.0	67	83	1	62.97	.512	.8486	GOOD
H7	109	1518	30000	THIN		13.0	60	83	2	37.19	.531	.7754	GOOD
H7	41	1017	17000	28000		10.0	41	83	0	39.98	.170	1.1766	POOR
H7	124	859	UNKN.	THIN	H	5.0	53	83	4	49.09	.391	1.0574	FAIR
H7	42	1103	20000	THIN		10.0	73	83	0	43.94	.691	.5310	GOOD
H7	42	1053	18000	22000		10.0	72	83	0	43.34	.685	.5475	GOOD
H7	124	809	UNKN.	THIN	H	5.0	34	84	2	38.42	.282	.8739	GOOD
H7	124	929	UNKN.	THIN	H	5.0	65	84	2	55.35	.567	.7436	GOOD
H7	42	1113	20000	THIN		10.0	73	84	0	44.42	.715	.4875	GOOD
H7	42	1123	UNKN.	THIN		10.0	73	84	0	44.78	.716	.4915	GOOD
H7	110	958	31000	33000	H	6.0	60	84	2	58.34	.517	.9357	GOOD
H7	42	1027	19000	27000		10.0	59	85	0	40.87	.583	.6279	FAIR
H7	42	1003	18000	20000		10.0	53	85	0	38.73	.440	.7352	POOR
H7	42	1143	UNKN.	THIN		10.0	73	85	0	45.11	.726	.5624	GOOD
H7	124	919	UNKN.	THIN	H	5.0	64	85	2	53.28	.565	.7563	GOOD

H7	124	909	UNKN.	THIN	H	5.0	62	85	2	51.19	.519	.8451	GOOD
H7	124	949	UNKN.	THIN	H	5.0	52	85	2	46.98	.373	1.1371	FAIR
H7	42	943	18000	20000		10.8	64	87	0	36.24	.577	.6442	FAIR
H7	41	1047	17000	28000		10.0	68	87	0	42.62	.714	.4980	FAIR
H7	124	759	UNKN.	THIN	H	5.0	49	93	2	36.27	.375	.9924	GOOD